Behavioral Expectations under Indeterminacy: An Empirical Evaluation*

Yasuo Hirose† Donghoon Yoo‡

October 15, 2025

Abstract

This paper investigates the quantitative implications and empirical relevance of behavioral expectations (BE) in dynamic stochastic general equilibrium (DSGE) models under equilibrium indeterminacy. Alongside the rational expectations (RE) benchmark, we examine two BE frameworks—diagnostic expectations (DE) and cognitive discounting (CD)—in both expectation formation and forecast error specifications. Using a simple example, we show that each combination yields a distinct equilibrium law of motion and different dynamic responses to fundamental and sunspot shocks. To evaluate their empirical relevance, we then estimate a medium-scale DSGE model for Japan's prolonged zero interest rate period, a likely episode of indeterminacy, under various BE specifications. The DE model with RE-based forecast errors outperforms other specifications in replicating key macroeconomic dynamics, particularly the overreaction of aggregate variables to major shocks. Variance and historical decompositions reveal technology and sunspot shocks as primary drivers of output and inflation, respectively. Sunspot shocks stabilize output but amplify inflation volatility. Relative to the RE benchmark, the DE model assigns greater importance to sunspot shocks, highlighting the role of BE and indeterminacy in Japan's macroeconomic fluctuations.

Keywords: Equilibrium indeterminacy, Diagnostic expectations, Cognitive discounting, Rational expectations, Bayesian estimation

JEL Classification Codes: C32, C62, E32, E71

*The authors would like to thank seminar participants at the Bank of Estonia for their comments and discussions. This study benefited from discussions with Jonathan Adams on solutions for behavioral expectations models and was supported by JSPS KAKENHI (24K00238, 25H00544) and a Korea University research grant (K2513021, K2528791). Yoo acknowledges the Bank of Estonia for its hospitality.

†Faculty of Economics, Keio University. Email: yhirose@econ.keio.ac.jp

‡Department of Economics, Korea University. Email: donghoonyoo@korea.ac.kr

1 Introduction

Dynamic Stochastic General Equilibrium (DSGE) models, which combine the optimizing behavior of forward-looking economic agents with market-clearing conditions, have become a central analytical tool not only in academic research but also in policy institutions such as central banks and international organizations. Despite their widespread use, most empirical applications of DSGE models focus exclusively on cases where the equilibrium is determinate—*i.e.*, uniquely determined by the model's structure and parameters—while disregarding the possibility of equilibrium indeterminacy.

However, several real-world features of fiscal and monetary policy, as well as macroeconomic data, suggest that the conditions under which indeterminacy arises in theory may in fact be relevant in practice. For instance, in Japan, the policy interest rate remained near zero for nearly a quarter of a century until August 2024, while inflation has recently trended upward amid global price increases. At the same time, the yen has depreciated steadily, partly due to negatively widening interest rate differentials with other economies. Standard DSGE models, when constructed to capture such environments, often lead to indeterminate equilibria, making them difficult to solve and estimate.[1] Consequently, there is a paucity of empirical research based on DSGE models that allow for indeterminacy, and it remains unclear how incorporating structural features that give rise to indeterminacy might affect the empirical implications of such models.

Standard DSGE models are typically solved under the assumption of rational expectations (RE), which serves as a useful benchmark for economic analysis. Nevertheless, the empirical plausibility of RE has been called into question, motivating a growing literature that relaxes this assumption in favor of behavioral expectations (BE). The literature has proposed various formulations of BE—such as adaptive expectations (Cagan, 1956; Friedman, 1957), sticky information (Mankiw and Reis, 2002), diagnostic expectations (DE) (Bordalo et al., 2020), cognitive discounting (CD) (Gabaix, 2020), and overextrapolation (Angeletos et al., 2020)—some of which can alter the conditions under which equilibria become indeterminate. However, the literature only focuses on the case where the equilibrium is determinate, and the properties of BE models under indeterminacy have not yet been explored. Besides, the majority of the existing studies remain theoretical, and to date, no empirical study has systematically examined which types of BE are most consistent with the data when indeterminacy is explicitly taken into account.

The objectives of this paper are twofold: (i) to establish the quantitative implications of BE models under indeterminacy; and (ii) to assess their empirical relevance. Specifically, in addition to RE, we consider and compare two types of BE: DE and CD, both of which are the most frequently analyzed quantitatively and empirically in the recent BE literature and exhibit contrasting dynamic

[1] In the prototypical New Keynesian model, equilibrium is indeterminate if the central bank does not adjust its policy rate more than one-for-one in response to inflation. Ascari and Ropele (2009) and Coibion and Gorodnichenko (2011) show that nonzero trend inflation makes the model more susceptible to indeterminacy. Beaudry and Lahiri (2019) and Fujiwara and Hirose (2024) demonstrate that equilibrium in a small open economy model can be indeterminate if the modified uncovered interest parity condition implies a negative relationship between expected exchange rate depreciation and interest rate differentials.

responses to fundamental shocks: overreaction and underreaction, respectively.[2]

Regarding the first objective, the literature typically solves BE models by representing the linearized system of equations using the RE operator, augmented with a parameter that captures the degree of deviation from RE. A standard linear RE solution method—such as those developed by Blanchard and Kahn (1980), Klein (2000), and Sims (2002)—can then be applied to derive the equilibrium law of motion for the endogenous variables. In this context, Adams (2023) points out that, under indeterminacy, the representation of the equilibrium solution in his general solution approach can vary depending on the specific formulation of BE and whether the associated forecast errors are defined based on RE or BE.

To examine the differences between the existing approach and that of Adams (2023), we illustrate solutions under indeterminacy both analytically and numerically using a simple univariate model. In this example, the solutions under determinacy coincide across the three distinct expectation formations: RE, DE, and CD. By contrast, under indeterminacy, each combination of expectation formation and forecast error specification yields a different law of motion for the endogenous variable and distinct dynamic responses to both fundamental and sunspot shocks. Moreover, the resulting solutions take different forms of vector autoregressive moving average (VARMA) processes with differing numbers of state variables, depending on whether forecast errors are assumed to be RE- or BE-based in the canonical representation of each model.

The second objective of this study is to estimate DSGE models with BE while allowing for indeterminacy, and to assess their empirical relevance using macroeconomic data. The novelty of this paper lies in its exploration of alternative BE frameworks and the evaluation of which formulations best align with the data under indeterminacy—an aspect largely overlooked in the existing empirical literature, which typically assumes determinacy. To the best of our knowledge, this is the first empirical study to estimate DSGE models featuring indeterminate equilibria under a range of expectation formation and forecast error specifications. This approach provides novel insights that are not attainable within the standard RE paradigm characterized by unique equilibria.

More specifically, we estimate medium-scale DSGE models for Japan's economy during the period of near-zero interest rates, which began in the late 1990s and lasted until 2024. During this time, the nominal interest rate was constrained by the zero lower bound, making it inappropriate to specify monetary policy using a Taylor-type rule that satisfies the Taylor principle. As a result, the equilibrium must be indeterminate. In addition to the RE benchmark, we consider two types of BE models—DE and CD—both of which are formulated with RE and corresponding BE forecast errors. We then compare the empirical performance of these models in terms of their fit to the data, their dynamic properties, and the sources of aggregate fluctuations during the period.

In the case of indeterminacy, an infinite number of equilibrium trajectories converge to the same

[2]For instance, Bianchi et al. (2024a), L'Huillier et al. (2024), and Na and Yoo (2025) estimate DSGE models incorporating DE, whereas Ilabaca et al. (2020), Meggiorini and Milani (2021), Meggiorini (2023), Afsar et al. (2024), Hirose et al. (2024), and Benchimol et al. (2025) estimate those with CD. These studies consider only cases in which equilibrium is determinate. A notable exception is Ilabaca and Meggiorini (2023), who estimate a New Keynesian model with nonzero trend inflation that incorporates CD in both the determinacy and indeterminacy regions of the model's parameter space.

steady state. Interpreting observed macroeconomic data as the realization of one particular path among many possible equilibrium trajectories, this study adopts a Bayesian estimation approach to identify the specific solution selected by the data. This approach, which we refer to as "equilibrium selection," enables the treatment of indeterminate models in the same way as determinate ones, allowing for meaningful empirical evaluation of their dynamic properties and overall plausibility. Moreover, under indeterminacy, sunspot shocks—*i.e.*, nonfundamental disturbances unrelated to macroeconomic fundamentals—can affect equilibrium dynamics. Our estimation strategy allows us to examine their contributions to observed macroeconomic fluctuations under different assumptions about expectation formation and forecast error specifications.

The estimation results demonstrate that the model incorporating DE with RE forecast errors delivers the best empirical performance among the five estimated specifications. Model comparison based on marginal data densities, autocorrelation functions, and model-implied covariance matrices consistently favors this specification, which closely replicates the observed time-series properties of Japan's macroeconomic data. The impulse response functions (IRFs) further indicate that the DE model captures realistic short-run dynamics—particularly the observed overreactions of aggregate variables to both fundamental and sunspot shocks—outperforming the benchmark RE model and other behavioral expectation variants.

The variance and historical decompositions reveal broadly similar results for the RE and DE models: technology shocks play the dominant role in driving output fluctuations, while sunspot shocks stabilize output during major downturns such as the global financial crisis and the COVID-19 pandemic. For inflation, however, sunspot shocks emerge as the primary driver and amplify volatility during turbulent periods. Relative to the RE model, the DE specification assigns a greater role to sunspot shocks, particularly in the historical decomposition of inflation, underscoring the empirical relevance of non-fundamental changes in BE for understanding Japan's business cycle dynamics under the prolonged zero interest rate regime.

The remainder of the paper proceeds as follows. Section 2 derives the solutions under RE and BE both analytically and numerically, using a simple univariate example. Section 3 describes the medium-scale DSGE model employed in the empirical analysis. Section 4 outlines the estimation strategy. Section 5 presents the estimation results. Section 6 concludes.

2 Solutions for Rational and Behavioral Expectations Systems Under Indeterminacy: A Simple Example

This section presents solutions for both RE and BE systems under indeterminacy—so-called sunspot solutions—using a simple linear univariate model. Following the literature, we solve BE models by representing them in terms of the RE operator, augmented by BE parameters that capture deviations from rationality. This formulation allows the application of standard algorithms developed for solving linear RE systems. To derive the complete set of linear solutions under indeterminacy, we adopt the approach of Lubik and Schorfheide (2003), who extended the method of Sims (2002)

to characterize an infinite number of equilibrium trajectories by incorporating an arbitrary matrix into the solution. In their framework, the system is expressed in a canonical form, augmented by the specification of forecast errors. If forecast errors are uniquely determined as functions of fundamental shocks by imposing non-explosive conditions, the equilibrium is determinate. Otherwise, it is indeterminate. Under indeterminacy, forecast errors are not fully pinned down by fundamentals, allowing sunspot shocks—non-fundamental disturbances to agents' expectations—to influence equilibrium dynamics.

In BE models, agents form expectations about the evolution of endogenous and exogenous variables based on behavioral heuristics rather than rational inference. The novelty of our approach lies in how we specify forecast errors within these behavioral frameworks, drawing inspiration from Adams (2023)'s general solution approach for a broad class of BE models. In addition to the standard forecast errors implied by RE, we introduce behavioral forecast errors, defined to be consistent with the underlying behavioral structure of the model. In the analysis that follows, we focus on two prominent BE models—DE and CD—both of which are widely discussed in the recent BE literature and generate contrasting dynamic responses to fundamental shocks: overreaction and underreaction, respectively. We demonstrate that behavioral distortions can lead to substantial differences in the form of solutions and generate richer dynamics under indeterminacy by leveraging BE-consistent forecast errors rather than RE-based ones as a solution device.

2.1 Analytical exploration

2.1.1 Rational expectations

Consider the following univariate linear RE model that characterizes the behavior of the endogenous variable y_t:

$$y_t = \frac{1}{\alpha}\mathbb{E}_t y_{t+1} + \varepsilon_t, \tag{1}$$

where $\mathbb{E}_t$ denotes the rational expectation operator, $\varepsilon_t \sim \ i.i.d.(0, \sigma_\varepsilon^2)$ is a fundamental shock, and α is a parameter. Following Sims (2002), we define an RE forecast error η_t:

$$\eta_t = y_t - \mathbb{E}_{t-1} y_t. \tag{2}$$

From (1) and (2), we obtain a dynamic equation for $\mathbb{E}_t y_{t+1}$:

$$\mathbb{E}_t y_{t+1} = \alpha \mathbb{E}_{t-1} y_t - \alpha\varepsilon_t + \alpha\eta_t. \tag{3}$$

Determinacy If $|\alpha| > 1$, nonexplosive conditions are given by $\mathbb{E}_0 y_1 = 0$ and $-\alpha\varepsilon_t + \alpha\eta_t = 0$ for all t, so that η_t is uniquely determined as a function of ε_t, *i.e.*, $\varepsilon_t = \eta_t$, leading to equilibrium

determinacy. Then, since $\mathbb{E}_t y_{t+1} = 0$ for all t, the solution for y_t under determinacy is given by

$$y_t = \varepsilon_t, \tag{4}$$

implying that y_t follows the i.i.d. process.

Indeterminacy Conversely, if $|\alpha| < 1$, the nonexplosive requirement imposes no restriction on the forecast error η_t. In this case, following Lubik and Schorfheide (2003), η_t can be expressed as a linear combination of the fundamental shock ε_t and a sunspot shock ζ_t:

$$\eta_t = \tilde{M}\varepsilon_t + M_\zeta \zeta_t, \tag{5}$$

where $\tilde{M}$ and M_ζ are arbitrary parameters unrelated to α. The sunspot shock ζ_t consists of nonfundamental disturbances to agents' expectations, including their self-fulfilling beliefs. Then, substituting (1) and (5) into (3), we obtain the solution for y_t under indeterminacy in the following ARMA(1,1) representation:

$$y_t = \alpha y_{t-1} + \tilde{M}\varepsilon_t - \alpha\varepsilon_{t-1} + M_\zeta \zeta_t. \tag{6}$$

Therefore, the sunspot solution (6) exhibits richer dynamics than the determinate solution given by (4).

2.1.2 Diagnostic expectations

Consider the same univariate model as in (1), but replace the RE operator with the DE operator:

$$y_t = \frac{1}{\alpha}\mathbb{E}_t^{DE} y_{t+1} + \varepsilon_t, \tag{7}$$

where $\mathbb{E}_t^{DE}$ denotes the DE operator. Since the exogenous shock ε_t is normally distributed, the future variable y_{t+1} also follows a normal distribution. Exploiting this Gaussian property, we can express the diagnostic expectation $\mathbb{E}_t^{DE} y_{t+1}$ in terms of the RE operator, as shown in Bordalo et al. (2018), Bianchi et al. (2024a), and L'Huillier et al. (2024):

$$\mathbb{E}_t^{DE} y_{t+1} = \mathbb{E}_t y_{t+1} + \theta\left(\mathbb{E}_t y_{t+1} - \mathbb{E}_{t-1} y_{t+1}\right),$$

where θ is a parameter that captures the degree of diagnosticity, reflecting the extent of deviation from rationality.[3] Substituting this expression into (7), we can rewrite the DE model in terms of

[3]Here, assume that the reference group used to compute the reference distribution is $t-1$ information set. However, the selective memory recall may also be based on more distant information sets. For instance, the diagnostic expectation of y_{t+1} with a distant memory can be formulated, as presented in Bianchi et al. (2024a) as

$$\mathbb{E}_t^{DE}[y_{t+1}] = \mathbb{E}_t[y_{t+1}] + \theta\left(\mathbb{E}_t[y_{t+1}] - \sum_{j=1}^{J}\alpha_j \mathbb{E}_{t-j}[y_{t+1}]\right),$$

the RE operator as:

$$y_t = \frac{1+\theta}{\alpha}\mathbb{E}_t y_{t+1} - \frac{\theta}{\alpha}\mathbb{E}_{t-1} y_{t+1} + \varepsilon_t. \tag{8}$$

Unlike RE models, this behavioral framework admits two plausible definitions of forecast errors: one may adopt RE-based forecast errors as a solution device, as is commonly assumed in the BE literature, or alternatively, employ BE-consistent forecast errors to solve the model.

Case 1: RE-based forecast errors

Suppose both the forecast error $\eta_{1,t}$ and forecast revision $\eta_{2,t}$ are defined under RE:

$$\eta_{1,t} = y_t - \mathbb{E}_{t-1} y_t, \tag{9}$$

$$\eta_{2,t} = \mathbb{E}_t y_{t+1} - \mathbb{E}_{t-1} y_{t+1}. \tag{10}$$

Substituting (9) into (8), the model can be written in the following canonical form that represents the joint dynamics of the expectational variables $\mathbb{E}_t y_{t+1}$ and $\mathbb{E}_t y_{t+2}$:

$$\begin{bmatrix} 1 & 0 \\ 1 & 0 \end{bmatrix} \begin{bmatrix} \mathbb{E}_t y_{t+1} \\ \mathbb{E}_t y_{t+2} \end{bmatrix} = \begin{bmatrix} \frac{\alpha}{1+\theta} & \frac{\theta}{1+\theta} \\ 0 & 1 \end{bmatrix} \begin{bmatrix} \mathbb{E}_{t-1} y_t \\ \mathbb{E}_{t-1} y_{t+1} \end{bmatrix} + \begin{bmatrix} -\frac{\alpha}{1+\theta} \\ 0 \end{bmatrix} \varepsilon_t + \begin{bmatrix} \frac{\alpha}{1+\theta} & 0 \\ 0 & 1 \end{bmatrix} \begin{bmatrix} \eta_{1,t} \\ \eta_{2,t} \end{bmatrix}. \tag{11}$$

Since the coefficient matrix on the left-hand side of the canonical system is singular, the stability of $\mathbb{E}_t y_{t+1}$ and $\mathbb{E}_t y_{t+2}$, as well as the condition for determinacy, can be analyzed by calculating the generalized eigenvalues of the system. As shown in Appendix A, the generalized eigenvalue is α, which coincides with that in the RE case (see Section 2.1.1). Therefore, the same determinacy condition applies in the DE case.

Determinacy If $|\alpha| > 1$, the nonexplosive condition implies that $\mathbb{E}_t y_{t+1} = 0$ and $\mathbb{E}_{t-1} y_{t+1} = 0$ for all t. Under this condition, from (8), the unique equilibrium solution for y_t is given by

$$y_t = \varepsilon_t,$$

which is identical to the solution in the RE case.

Indeterminacy Due to the aforementioned singularity, the equilibrium solution can no longer be derived analytically. In what follows, we implicitly characterize the solution in matrix form.

If $|\alpha| < 1$, the stability condition does not fully determine $\eta_{1,t}$ and $\eta_{2,t}$ as functions of ε_t. Accordingly, the vector of the forecast error and forecast revision, denoted by $\eta_t \equiv [\eta_{1,t}, \eta_{2,t}]'$, can be expressed as

$$\eta_t = M(\alpha, \theta, \tilde{M})\varepsilon_t + M_\zeta \zeta_t,$$

where α_j represents the weight attached to the expectation at time $t-j$ and $J > 1$.

where M is a conformable vector that depends on the structural parameters α and θ, as well as an arbitrary parameter $\tilde{M}$, and M_ζ denotes an arbitrary coefficient vector associated with the sunspot shock ζ_t. The dimension of the sunspot shock is normalized to one. Incorporating y_t into the vector of endogenous variables, the resulting sunspot solution takes the form:

$$\begin{bmatrix} y_t \\ \mathbb{E}_t y_{t+1} \\ \mathbb{E}_t y_{t+2} \end{bmatrix} = A(\alpha,\theta) \begin{bmatrix} y_{t-1} \\ \mathbb{E}_{t-1} y_t \\ \mathbb{E}_{t-1} y_{t+1} \end{bmatrix} + B(\alpha,\theta,\tilde{M})\varepsilon_t + C(\alpha,\theta,M_\zeta)\zeta_t. \tag{12}$$

A notable feature of the DE solution is that both the fundamental shock ε_t and the sunspot shock ζ_t influence equilibrium dynamics not only contemporaneously, but also with a lag. They affect the system on impact through $\mathbb{E}_t y_{t+1}$, and with a one-period lag via $\mathbb{E}_{t-1} y_t$ and $\mathbb{E}_{t-1} y_{t+1}$, the latter serving as the lagged expectation of $\mathbb{E}_t y_{t+2}$.

Case 2: BE-based forecast errors

We now exploit the notion of DE-based forecast errors in solving the system. For $\mathbb{E}_t^{DE} y_{t+1}$ in the original model (1), a DE-based forecast error is defined as

$$\eta_{1,t} = y_t - \mathbb{E}_{t-1}^{DE} y_t,$$

so that, in terms of the RE operator,

$$\eta_{1,t} = y_t - (1+\theta)\mathbb{E}_{t-1} y_t + \theta \mathbb{E}_{t-2} y_t. \tag{13}$$

Substituting (13) into (8), we have

$$\mathbb{E}_t y_{t+1} = \alpha \mathbb{E}_{t-1} y_t + \frac{\theta}{1+\theta}\mathbb{E}_{t-1} y_{t+1} - \frac{\alpha\theta}{1+\theta}\mathbb{E}_{t-2} y_t - \frac{\alpha}{1+\theta}\varepsilon_t + \frac{\alpha}{1+\theta}\eta_{1,t}.$$

Then, together with the definition of the forecast revision $\eta_{2,t}$ given by (10)[4] and an auxiliary identity equation $\mathbb{E}_{t-1} y_{t+1} = \mathbb{E}_{t-1} y_{t+1}$, the model can be written in the following canonical form for the expectational variables $\mathbb{E}_t y_{t+1}$, $\mathbb{E}_t y_{t+2}$, and $\mathbb{E}_{t-1} y_{t+1}$:

$$\begin{bmatrix} 1 & 0 & 0 \\ 1 & 0 & 0 \\ 0 & 0 & 1 \end{bmatrix} \begin{bmatrix} \mathbb{E}_t y_{t+1} \\ \mathbb{E}_t y_{t+2} \\ \mathbb{E}_{t-1} y_{t+1} \end{bmatrix} = \begin{bmatrix} \alpha & \frac{\theta}{1+\theta} & -\frac{\alpha\theta}{1+\theta} \\ 0 & 1 & 0 \\ 0 & 1 & 0 \end{bmatrix} \begin{bmatrix} \mathbb{E}_{t-1} y_t \\ \mathbb{E}_{t-1} y_{t+1} \\ \mathbb{E}_{t-2} y_t \end{bmatrix} + \begin{bmatrix} -\frac{\alpha}{1+\theta} \\ 0 \\ 0 \end{bmatrix} \varepsilon_t + \begin{bmatrix} \frac{\alpha}{1+\theta} & 0 \\ 0 & 1 \\ 0 & 0 \end{bmatrix} \begin{bmatrix} \eta_{1,t} \\ \eta_{2,t} \end{bmatrix}. \tag{14}$$

As in the case with RE-based forecast errors, the coefficient matrix on the left-hand side of the canonical system is singular. Consequently, the stability properties of the system, as well as the determinacy condition, can be analyzed using the system's generalized eigenvalues. As shown in Appendix A, these eigenvalues are 0 and α. The zero eigenvalue reflects the unit root associated

[4]The forecast revision is defined under RE because the related variable, *i.e.*, $\mathbb{E}_{t-1} y_{t+1}$, appears only in the RE representation of the model.

with the identity equation for $\mathbb{E}_{t-1}y_{t+1}$, implying that system stability depends solely on α, as in the RE case (see Section 2.1.1). Therefore, the same determinacy condition applies in this setting.

Determinacy If $|\alpha| > 1$, then, for the same reason as in the case with RE-based forecast errors, the unique equilibrium solution for y_t is given by

$$y_t = \varepsilon_t,$$

which is identical to the solution in the RE case.

Indeterminacy If $|\alpha| < 1$, the stability requirement cannot fully pin down $\eta_{1,t}$ and $\eta_{2,t}$ as functions of ε_t. As in the RE-based forecast error case, the forecast error and revision $\eta_t \equiv [\eta_{1,t}, \eta_{2,t}]'$ are given by

$$\eta_t = M(\alpha, \theta, \tilde{M})\varepsilon_t + M_\zeta \zeta_t.$$

Including y_t into the vector of endogenous variables, the sunspot solution takes the following form:

$$\begin{bmatrix} y_t \\ \mathbb{E}_t y_{t+1} \\ \mathbb{E}_t y_{t+2} \\ \mathbb{E}_{t-1} y_{t+1} \end{bmatrix} = A(\alpha, \theta) \begin{bmatrix} y_{t-1} \\ \mathbb{E}_{t-1} y_t \\ \mathbb{E}_{t-1} y_{t+1} \\ \mathbb{E}_{t-2} y_t \end{bmatrix} + B(\alpha, \theta, \tilde{M})\varepsilon_t + C(\alpha, \theta, M_\zeta)\zeta_t. \tag{15}$$

Hence, the propagation of shocks can be more persistent than in the RE-based forecast error case. Specifically, shocks affect the equilibrium dynamics on impact via $\mathbb{E}_t y_{t+1}$; with a one-period lag through $\mathbb{E}_{t-1}y_t$ and $\mathbb{E}_{t-1}y_{t+1}$ (which corresponds to the one-period lag of $\mathbb{E}_t y_{t+2}$); and with a two-period lag through $\mathbb{E}_{t-2}y_t$ (the two-period lag of $\mathbb{E}_t y_{t+2}$).

2.1.3 Cognitive discounting

Consider the same model, but under CD:

$$y_t = \frac{1}{\alpha}\mathbb{E}_t^{CD} y_{t+1} + \varepsilon_t, \tag{16}$$

where $\mathbb{E}_t^{CD}$ denotes the expectation operator under CD. Following Gabaix (2020), the CD expectation can be represented in terms of the RE operator as:

$$\mathbb{E}_t^{CD} y_{t+1} = \phi \mathbb{E}_t y_t, \tag{17}$$

where the parameter ϕ captures the degree of CD.[5] We consider $0 < \phi < 1$ to remain consistent with the microfoundation of CD proposed by Gabaix (2020).[6] Substituting (17) into (16), the model can be rewritten using the RE operator as:

$$y_t = \frac{\phi}{\alpha}\mathbb{E}_t y_{t+1} + \varepsilon_t. \tag{18}$$

As in the earlier discussion of the solutions under DE (see Section 2.1.2), there are two plausible ways to incorporate a forecast error regarding $\mathbb{E}_t y_{t+1}$ when solving the system: using an RE-based forecast error or a BE-based forecast error consistent with CD.

Case 1: RE-based forecast error

When the forecast error is defined under RE, as in (2), the model (18) can be expressed as a dynamic equation for $\mathbb{E}_t y_{t+1}$:

$$\mathbb{E}_t y_{t+1} = \frac{\alpha}{\phi}\mathbb{E}_{t-1} y_t + \frac{\alpha}{\phi}\eta_t - \frac{\alpha}{\phi}\varepsilon_t. \tag{19}$$

This equation indicates that, in contrast to the benchmark RE model discussed in Section 2.1.1, the stability of $\mathbb{E}_t y_{t+1}$—and hence the condition for determinacy—is governed by the ratio α/ϕ, rather than by α alone.

Determinacy If $|\alpha/\phi| > 1$, the nonexplosive condition implies that $\mathbb{E}_t y_{t+1} = 0$ for all t. Under this condition, the unique equilibrium solution for y_t, derived from (18), coincides with that of the RE case:

$$y_t = \varepsilon_t.$$

Indeterminacy By contrast, when $|\alpha/\phi| < 1$, the stability condition imposes no restriction on the RE forecast error η_t. In this case, η_t can be expressed as a linear combination of the fundamental shock ε_t and a sunspot shock ζ_t:

$$\eta_t = \tilde{M}\varepsilon_t + M_\zeta \zeta_t,$$

where $\tilde{M}$ and M_ζ are free parameters, independent of α and ϕ. Substituting this expression into (19), together with (18), yields the sunspot solution for y_t:

$$y_t = \frac{\alpha}{\phi} y_{t-1} + \tilde{M}\varepsilon_t - \frac{\alpha}{\phi}\varepsilon_{t-1} + M_\zeta \zeta_t. \tag{20}$$

[5] For this RE representation to hold, Gabaix (2020) assumes that behavioral agents are rational with respect to the steady state but myopic with regard to deviations from it. In the current model, we consider y_t as a deviation from its steady state.

[6] Angeletos et al. (2020) allow for both $\phi > 1$ and $0 < \phi < 1$ to capture over- and under-extrapolation, respectively.

This solution follows an ARMA(1,1) process similar to the sunspot solution (6) under RE, but with different coefficients on the lagged variables y_{t-1} and ε_{t-1}.

Case 2: BE-based forecast error

Suppose the forecast error is defined in a manner consistent with how expectations are formed under CD:

$$\eta_t = y_t - \mathbb{E}_{t-1}^{CD} y_t,$$

which, when expressed using the RE operator, becomes:

$$\eta_t = y_t - \phi \mathbb{E}_{t-1} y_t. \tag{21}$$

Substituting (21) into the RE representation of the model (18), we obtain the following dynamic equation for $\mathbb{E}_t y_{t+1}$:

$$\mathbb{E}_t y_{t+1} = \alpha \mathbb{E}_{t-1} y_t + \frac{\alpha}{\phi} \eta_t - \frac{\alpha}{\phi} \varepsilon_t. \tag{22}$$

Unlike the case with the RE-based forecast error, the stability of the system here is determined solely by α. Accordingly, the condition for determinacy coincides with that in the RE model (see Section 2.1.1).

Determinacy Consequently, if $|\alpha| > 1$, the stability condition requires that $\mathbb{E}_t y_{t+1} = 0$ for all t, leading to the unique equilibrium solution for y_t:

$$y_t = \varepsilon_t.$$

Therefore, under determinacy, the solution is identical across all specifications of expectation formation and forecast error assumptions.

Indeterminacy On the other hand, if $|\alpha| < 1$, the stability condition imposes no restriction on the CD-based forecast error η_t. As in the case with the RE-based forecast error, it can then be specified as:

$$\eta_t = \tilde{M} \varepsilon_t + M_\zeta \zeta_t.$$

Substituting this expression into (22) and combining it with (18), we obtain the sunspot solution of the form:

$$y_t = \alpha y_{t-1} + \tilde{M} \varepsilon_t - \alpha \varepsilon_{t-1} + M_\zeta \zeta_t,$$

which coincides with the solution (4) in the benchmark RE model under indeterminacy. However, this equivalence does not necessarily imply that the CD model with CD-based forecast errors generally yields the same solution as its RE counterpart across broader classes of linear systems. As demonstrated in the subsequent empirical analysis, the medium-scale DSGE model produces distinct equilibrium solutions—and thus different estimation outcomes—depending on the specification of expectation formation and the associated forecast error assumptions.

2.2 Internal propagation under indeterminacy

A distinctive theoretical implication of the DE model—namely, overreaction followed by a predictable reversal—arises only in the presence of either (i) persistent exogenous shocks (exogenous persistence) or (ii) predetermined endogenous variables (endogenous persistence). This argument holds under equilibrium determinacy. Indeed, in the simple univariate example above, the explicit solution for y_t under determinacy is given by $y_t = \varepsilon_t$, which coincides exactly with the solution of the RE counterpart, regardless of the assumptions on expectation formation and forecast errors.

However, under indeterminacy, the DE model can yield distinct equilibrium solutions—and hence exhibit distinctive dynamic properties—even in the absence of persistent exogenous shocks or predetermined endogenous variables. This offers a novel internal propagation mechanism within linear DSGE models. Specifically, although explicit solutions cannot be derived, the implicit solutions given in (12) and (15) follow VARMA processes augmented with lagged expectational terms, resulting in richer dynamics than those under the RE specification.

As for the CD model, while the solution under the CD-based forecast error coincides with its RE counterpart, the solution in (20) under the RE-based forecast error amplifies the influence of lagged endogenous variables and fundamental shocks, provided that $0 < \phi < 1$. This result stands in stark contrast to the conventional under-reaction property of CD models under determinacy. In such models, the contemporaneous propagation of shocks is generally dampened because the CD factor reduces the weight assigned to future outcomes and increases the relative importance of past variables. Under indeterminacy, however, the solution becomes more backward-looking, thereby enhancing internal propagation from past states.

2.3 Numerical Illustration

In Section 2.1, while we derive the sunspot solutions to the simple univariate model analytically under RE and CD, we characterize them only implicitly in matrix form under DE. To compare the dynamic properties of the solutions across different specifications of expectation formation and forecast errors, we compute the solutions numerically and illustrate the IRFs to the fundamental and sunspot shocks under indeterminacy. For illustration purposes, we set the model's parameters as follows: $\alpha = 0.75$, $\theta = 0.9$, and $\phi = 0.9$. Regarding the arbitrary parameters in the sunspot solutions—which select particular equilibria under indeterminacy—we fix $\tilde{M} = 0$ and $M_\zeta = 1$, with

Figure 1: Impulse Responses: (a) Fundamental Shocks; and (b) Sunspot Shocks

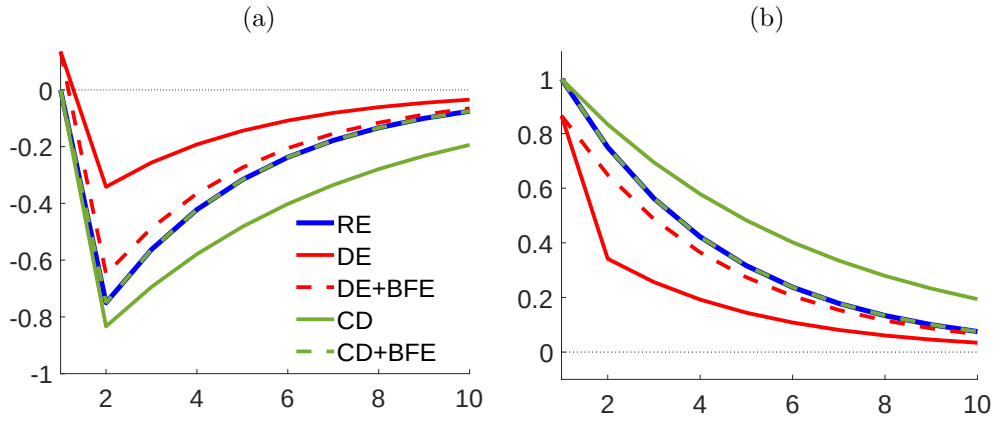

Notes: This figure displays the responses of y_t to one-unit positive increases in (a) fundamental shocks and (b) sunspot shocks in the simple univariate models under five alternative specifications: the RE model, the DE model with RE forecast errors (DE), the DE model with DE forecast errors (DE+BFE), the CD model with RE forecast errors (CD), and the CD model with CD forecast errors (CD+BFE). For all specifications, the parameters are set as follows: $\alpha = 0.75$, $\theta = 0.9$, $\phi = 0.9$, $\tilde{M} = 0$, and $M_\zeta = 1$.

the dimension of the sunspot shocks normalized to one.[7]

Figure 1 plots the IRFs of the endogenous variable y_t to one-unit increases in the fundamental shock (left panel) and the sunspot shock (right panel) in the univariate models under five alternative specifications: the RE model (blue solid lines), the DE model with RE forecast errors (red solid lines), the DE model with DE forecast errors (red dashed lines), the CD model with RE forecast errors (green solid lines), and the CD model with CD forecast errors (green dashed lines). There are three notable differences and similarities across these specifications.

First, among these five models, only the DE models (red solid and dashed lines)—regardless of whether forecast errors are based on RE or BE—exhibit a positive immediate response of y_t to the fundamental shock, highlighting the overreaction feature of DE models. The right panel further shows that the DE model with RE forecast errors (red solid line) displays a distinctive response to the sunspot shock: the effect diminishes sharply in the second period but thereafter remains more persistent than in the other specifications. The sharp decline reflects the typical overreaction-and-reversal property of DE models, while the subsequent greater persistence arises from the solution form in (20), which includes lagged expectations as additional state variables, thereby inducing more persistent dynamics.

Second, the responses of y_t in the CD model with CD forecast errors (green dashed lines) are identical to those under RE (blue solid lines) for both fundamental and sunspot shocks, as also shown analytically in Section 2.1.3. However, incorporating BE forecast errors does not, in

[7]The sunspot solution with $\tilde{M} = 0$ and $M_\zeta = 1$ corresponds to the particular solution obtained by the GENSYS algorithm of Sims (2002). In the subsequent empirical analysis, we estimate arbitrary parameters in $\tilde{M}$ in a medium-scale DSGE model.

general, eliminate behavioral distortions. For instance, compare the responses under DE with DE forecast errors (red dashed lines) to those under RE (blue lines). Moreover, as demonstrated by the empirical evaluation using a medium-scale DSGE model in the next section, the dynamics under CD with CD forecast errors do not always coincide with those under RE, due to the presence of endogenous lagged state variables. In addition, the current figure shows that the responses under CD with RE forecast errors (green solid lines) exhibit greater persistence than those under the RE benchmark, consistent with the discussion in Section 2.1.3.

Third, comparing the responses in the BE models with different forecast error specifications—the DE model with RE forecast errors (red solid lines) versus the DE model with DE forecast errors (red dashed lines), and the CD model with RE forecast errors (green solid lines) versus the CD model with CD forecast errors (green dashed lines)—we find that the way forecast errors are defined in a behavioral system critically affects the system's dynamics. In both the DE and CD models, the responses of y_t differ significantly from those in the RE model (blue lines) when forecast errors are specified based on RE. Conversely, when forecast errors are defined under BE, the responses more closely resemble their RE counterparts.

3 The Model

Building on the theoretical findings from the previous section, we conduct an empirical evaluation of BE and forecast error specifications within a richer DSGE framework. Our primary objective is to assess whether the introduction of BE improves the model's ability to fit macroeconomic time series in an environment characterized by equilibrium indeterminacy.

Guided by this broad question, our empirical analysis addresses several subquestions: What are the estimated values of the key structural BE parameters on DE and CD? Do their credible intervals include the RE limit? How important is the specification of forecast errors in BE models? Do RE-based forecast error specifications provide a better fit to the data, or is the opposite true? More importantly, is there statistical evidence that BE models better replicate Japan's business cycles during its prolonged zero interest rate period?

To better evaluate the role of expectation channels under indeterminacy, our empirical model incorporates a range of competing frictions and shocks. In addition, to capture the business cycle dynamics of the Japanese economy, we introduce several modifications to the standard medium-scale DSGE model, developed by Christiano et al. (2005), Smets and Wouters (2007), and Justiniano et al. (2010). The inclusion of commonly used nominal and real frictions, along with various driving processes, allows for a rigorous assessment of the behavioral frictions embedded in the DE and CD models under the more empirically realistic setting.

3.1 Medium-scale DSGE model

The model is a medium-scale DSGE model based on the framework of Hirose (2020), sharing many features with Christiano et al. (2005), Smets and Wouters (2007), and Justiniano et al. (2010), but

differing in two key respects. First, households' preferences follow Erceg et al. (2006), ensuring the existence of a balanced growth path under a constant relative risk aversion (CRRA) utility function. Second, following Greenwood et al. (1988), the model assumes that a higher capital utilization rate leads to a higher capital depreciation rate. This assumption is supported by Sugo and Ueda (2008), who estimate a Christiano et al. (2005)-type model for the Japanese economy under the same assumption and successfully replicate a negative correlation between capital utilization and rental cost observed in the data.

To incorporate BE, we modify Hirose (2020)'s model by replacing Calvo (1983)-type staggered price and wage settings with Rotemberg (1982)-type price and wage adjustment costs. This modification considerably simplifies the RE representation of the New Keynesian price and wage Phillips curves under BE. In addition, we omit wage indexation in order to avoid possible unit-root processes in the case of DE with DE-based forecast errors.

In the model economy, there is a continuum of households, a representative final-good firm, a continuum of intermediate-good firms, and a central bank. Their optimization problems and setups are presented below, while the corresponding first-order conditions are shown in Appendix B.1. In the description of the model, $\mathbb{E}_t^*$ denotes the expectations operator at time t that allows for either RE or BE. We formulate dynamic optimization problems by explicitly separating time-t choice variables from the expectations of future choice variables. This separation is essential for solving certain models under BE with path dependence.[8]

3.1.1 Households

There is a continuum of households $h \in [0,1]$, each of which purchases consumption goods $C_t(h)$ and one-period riskless bonds $B_t(h)$, and supplies one kind of differentiated labor service $l_t(h)$ to intermediate-good firms. Each household's preferences are represented by the utility function:

$$e^{z_t^b}\left(\frac{(C_t(h)-\gamma C_{t-1}(h))^{1-\sigma}}{1-\sigma}-\frac{Z_t^{1-\sigma}l_t(h)^{1+\chi}}{1+\chi}\right)$$
$$+\mathbb{E}_t^*\sum_{j=1}^{\infty}\beta^j e^{z_{t+j}^b}\left\{\frac{(C_{t+j}(h)-\gamma C_{t+j-1}(h))^{1-\sigma}}{1-\sigma}-\frac{Z_{t+j}^{1-\sigma}l_{t+j}(h)^{1+\chi}}{1+\chi}\right\},$$

where $\beta \in (0,1)$ is the subjective discount factor, $\sigma > 0$ measures the degree of risk aversion, $\gamma \in [0,1]$ represents the degree of habit persistence in consumption preferences, $\chi > 0$ is the inverse of the labor supply elasticity, Z_t represents the level of neutral technology, and z_t^b denotes a shock to the subjective discount factor. As in Erceg et al. (2006), we assume the presence of $Z_t^{1-\sigma}$ in the disutility of labor, which ensures the existence of a balanced growth path in the model economy.

In monopolistically competitive labor markets, wages $W_t(h)$ are chosen in the face of labor demand given by $l_t(h) = l_t(W_t(h)/W_t)^{-(1+\lambda_t^w)/\lambda_t^w}$, where $l_t = \left\{\int_0^1 l_t(h)^{1/(1+\lambda_t^w)}dh\right\}^{1+\lambda_t^w}$ and $\lambda_t^w > 0$ is related to the substitution elasticity between differentiated labor services and represents the

[8] See, for example, L'Huillier et al. (2024) for such a treatment under DE.

exogenous time-varying wage markup.

At the beginning of each period, each household owns a capital stock $K_{t-1}(h)$ and rents utilization-adjusted capital $u_t(h)K_{t-1}(h)$ to intermediate-good firms at the real rental price $R_t^k(h)$. Then, the capital utilization rate $u_t(h)$ and investment spending $I_t(h)$ are determined subject to the capital accumulation equation:

$$K_t(h) = \{1 - \delta(u_t(h))\} K_{t-1}(h) + e^{z_t^i} \left\{ 1 - S\left(\frac{I_t(h)}{I_{t-1}(h)z} \right) \right\} I_t(h).$$

Here, following Greenwood et al. (1988), the model assumes that a higher utilization rate of capital leads to a higher depreciation rate of capital. Hence, the depreciation rate function $\delta(\cdot)$ has the properties $\delta' > 0$, $\delta'' > 0$, $\delta(u) = \delta \in (0,1)$, and $\mu = \delta'(u)/\delta''(u) > 0$, where $u = 1$ is the steady-state capital utilization rate. The function $S(\cdot)$ represents the costs involved in changing investment spending, such as financial intermediation costs analyzed in Carlstrom and Fuerst (1997), and takes the quadratic form of $S(x) = \varphi_i(x-1)^2/2$, where φ_i is a positive constant. The variable z_t^i is a shock to the marginal efficiency of investment (MEI). The parameter $z > 1$ represents the gross balanced growth rate.

Each household's budget constraint is given by

$$\begin{aligned} C_t(h) + I_t(h) + \frac{B_t(h)}{P_t} = {} & W_t(h)l_t(h) + R_t^k(h)u_t(h)K_{t-1}(h) + R_{t-1}^n \frac{B_{t-1}(h)}{P_t} + T_t(h) \\ & - \frac{\varphi_w}{2} \left\{ \frac{P_t W_t(h)}{P_{t-1}W_{t-1}(h)\pi z} - 1 \right\}^2 W_t(h)l_t(h), \end{aligned}$$

where P_t is the price of final goods, $W_t(h)$ is the real wage, R_t^n is the gross nominal interest rate and $T_t(h)$ consists of net public transfers and profits received from firms. The last term captures Rotemberg-type wage adjustment costs that each household incurs when a change in nominal wage deviates from its steady-state value. $\varphi_w > 0$ is the parameter governing the adjustment costs, *i.e.*, the degree of nominal wage stickiness.

3.1.2 Firms

Final-good firm The final-good firm produces output Y_t by choosing a combination of intermediate inputs $\{Y_t(f)\}$, with $f \in [0,1]$, so as to maximize its profit:

$$P_t Y_t - \int_0^1 P_t(f) Y_t(f) df,$$

subject to the aggregator:

$$Y_t = \left\{ \int_0^1 Y_t(f)^{1/(1+\lambda_t^p)} df \right\}^{1+\lambda_t^p},$$

where $P_t(f)$ is the price of intermediate good f, and $\lambda_t^p > 0$ is related to the substitution elasticity between differentiated goods and corresponds to the exogenous, time-varying price markup.

The market clearing condition for the final good is

$$Y_t = C_t + I_t + dZ_t e^{z_t^d} + \frac{\varphi_p}{2}\left(\frac{\pi_t}{\pi_{t-1}^{\gamma_p}\pi^{1-\gamma_p}} - 1\right)^2 Y_t,$$

where the term $dZ_t e^{z_t^d}$ represents an external demand component that consists of government spending and net exports. Here, z_t^d is an external demand shock, and d is a scale parameter. The last term captures aggregate price adjustment costs.

Intermediate-good firms Each intermediate-good firm f produces output $Y_t(f)$ by choosing a cost-minimizing pair of capital and labor services $\{u_t K_{t-1}(f), l_t(f)\}$, given their real prices (R_t^k, W_t) and the production function:

$$Y_t(f) = (Z_t l_t(f))^{1-\alpha} (u_t K_{t-1}(f))^{\alpha} - \varphi_y Z_t. \tag{23}$$

Here, Z_t represents the level of neutral technology and is assumed to follow the stochastic process:

$$\log Z_t = \log z + \log Z_{t-1} + z_t^z, \tag{24}$$

where $z > 1$ is the steady-state gross rate of neutral technological change, and z_t^z represents a shock to the rate of this change. The parameter $\alpha \in (0, 1)$ measures the capital elasticity of output. The last term in the production function (23), $-\varphi_y Z_t$, is the fixed cost of producing intermediate goods, and φ_y is a positive constant.[9]

Aggregating the production function (23) over intermediate-good firms yields

$$Y_t d_t = (Z_t l_t)^{1-\alpha} (u_t K_{t-1})^{\alpha} - \varphi_y Z_t,$$

where $d_t = \int_0^1 (P_t(f)/P_t)^{-(1+\lambda_t^p)/\lambda_t^p} df$ measures the intermediate-good price dispersion and is a second-order term under the staggered price setting presented below.

Facing the final-good firm's demand, each intermediate-good firm maximizes its profit by setting the price of its product while incurring Rotemberg-type adjustment costs when its price change

[9] The zero profit condition for intermediate-good firms at the steady state leads to $\varphi_y = \lambda^p$, where λ^p is the steady-state price markup.

deviates from a weighted average of its aggregate past and steady-state changes:

$$\max_{P_t(f)} \left\{ \frac{P_t(f)}{P_t} - mc_t - \frac{\varphi_p}{2} \left(\frac{\frac{P_t(f)}{P_{t-1}(f)}}{\pi_{t-1}^{\gamma_p} \pi^{1-\gamma_p}} - 1 \right)^2 \right\} Y_t(f) +$$
$$\mathbb{E}_t^* \sum_{j=1}^{\infty} \beta^j \frac{\Lambda_{t+j}}{\Lambda_t} \left\{ \frac{P_{t+j}(f)}{P_{t+j}} - mc_{t+j} - \frac{\varphi_p}{2} \left(\frac{\frac{P_{t+j}(f)}{P_{t+j-1}(f)}}{\pi_{t+j-1}^{\gamma_p} \pi^{1-\gamma_p}} - 1 \right)^2 \right\} Y_{t+j}(f),$$

subject to

$$Y_t(f) = Y_t \left(\frac{P_t(f)}{P_t} \right)^{-\frac{1+\lambda_t^p}{\lambda_t^p}},$$

where $\varphi_p > 0$ is the parameter governing the adjustment costs, measuring the degree of price stickiness, and $\gamma_p \in [0, 1]$ is the weight of price indexation to past inflation relative to steady-state inflation.

3.1.3 Central bank

Taking into account the fact that the nominal interest rate setting is constrained by the zero lower bound, the monetary policy can no longer be described using a Taylor-type monetary policy rule. Instead, the nominal interest rate is assumed to follow the first-order autoregressive process:

$$\tilde{R}_t^n = \psi_r \tilde{R}_{t-1}^n + \varepsilon_t^r, \tag{25}$$

where $\tilde{R}_t^n$ represents the percentage deviation of the nominal interest rate from its steady state, ε_t^r is a monetary policy shock, and $\psi_r \in [0, 1)$ is the degree of policy rate smoothing.[10] Then, the monetary policy does not react to inflation anymore and hence cannot satisfy the Taylor principle.

3.1.4 Fundamental shock processes

The model contains seven fundamental shocks; *i.e.*, technology z_t^z, preference z_t^b, marginal efficiency of investment (MEI) z_t^i, external demand z_t^d, wage markup z_t^w, price markup z_t^p, and monetary policy ε_t^r shocks. While the monetary policy shock $\varepsilon_t^r \sim i.i.d.N(0, \sigma_r^2)$, the other shocks follow stationary first-order autoregressive processes:

$$z_t^x = \rho_x z_{t-1}^x + \varepsilon_t^x, \quad \varepsilon_t^x \sim i.i.d.N(0, \sigma_x^2)$$

where $\rho_x \in [0, 1)$ and $x \in \{z, b, i, d, w, p\}$.

[10] Another possible specification for the nominal interest rate is to exogenously fix it at zero or its effective lower bound. However, this paper employs a stochastic process for the nominal interest rate to reflect the fact that the Bank of Japan changed the policy rate from virtually zero during the periods of August 2000–March 2001 and July 2006–December 2008.

3.2 System of equilibrium conditions

In the model, the real variables are nonstationary because the level of neutral technology has a unit root with drift as shown in (24). Thus, we rewrite the equilibrium conditions in terms of stationary variables detrended by Z_t; *i.e.*, $y_t = Y_t/Z_t$, $c_t = C_t/Z_t$, $w_t = W_t/Z_t$, $\lambda_t = \Lambda_t Z_t^{\sigma}$, $i_t = I_t/Z_t$, $k_t = K_t/Z_t$, and $z_{t+1} = Z_{t+1}/Z_t$, so that we can compute the steady states for the detrended variables. The detrended equilibrium conditions and steady-state relationships are presented in Appendix B.2.

3.2.1 Rational expectations

Let $\mathbb{E}_t$ denote the RE operator. Then, log-linearizing the detrended equilibrium conditions around the steady state leads to the following linear system of equations:

$$\left(1-\frac{\beta\gamma}{z^{\sigma}}\right)\tilde{\lambda}_t = -\frac{\sigma z}{z-\gamma}\left\{\tilde{c}_t - \frac{\gamma}{z}\left(\tilde{c}_{t-1} - z_t^z\right)\right\} + z_t^b + \frac{\beta\gamma}{z^{\sigma}}\left\{\frac{\sigma z}{z-\gamma}\left(\mathbb{E}_t\tilde{c}_{t+1} + \mathbb{E}_t z_{t+1}^z - \frac{\gamma}{z}\tilde{c}_t\right) - \mathbb{E}_t z_{t+1}^b\right\} \tag{26}$$

$$\tilde{\lambda}_t = \mathbb{E}_t\tilde{\lambda}_{t+1} - \sigma\mathbb{E}_t z_{t+1}^z + \tilde{R}_t^n - \mathbb{E}_t\tilde{\pi}_{t+1} \tag{27}$$

$$\tilde{\pi}_t + \tilde{w}_t - \tilde{w}_{t-1} + z_t^z = \beta z^{1-\sigma}\left\{\tilde{\pi}_{t+1} + \mathbb{E}_t\tilde{w}_{t+1} - \tilde{w}_t + \mathbb{E}_t z_{t+1}^z\right\} + \frac{1}{\varphi_w\lambda^w}\left(\chi\tilde{l}_t - \tilde{\lambda}_t - \tilde{w}_t + z_t^b\right) + z_t^w \tag{28}$$

$$\tilde{u}_t = \mu\left(\tilde{r}_t^k - \tilde{q}_t\right) \tag{29}$$

$$\varphi_i\left(\tilde{\imath}_t - \tilde{\imath}_{t-1} + z_t^z\right) = \tilde{q}_t + \beta z^{1-\sigma}\varphi_i\left(\mathbb{E}_t\tilde{\imath}_{t+1} - \tilde{\imath}_t + \mathbb{E}_t z_{t+1}^z\right) + z_t^i \tag{30}$$

$$\tilde{q}_t = \mathbb{E}_t\tilde{\lambda}_{t+1} - \tilde{\lambda}_t - \sigma\mathbb{E}_t z_{t+1}^z + \frac{\beta}{z^{\sigma}}\left\{R^k\mathbb{E}_t\tilde{R}_{t+1}^k + (1-\delta)\mathbb{E}_t\tilde{q}_{t+1}\right\} \tag{31}$$

$$\tilde{k}_t = \frac{1-\delta}{z}\left(\tilde{k}_{t-1} - z_t^z\right) + \frac{R^k}{z}\tilde{u}_t + \left(1 - \frac{1-\delta}{z}\right)\tilde{\imath}_t \tag{32}$$

$$\tilde{y}_t = \frac{c}{y}\tilde{c}_t + \frac{i}{y}\tilde{\imath}_t + \frac{d}{y}z_t^d \tag{33}$$

$$\tilde{mc}_t = (1-\alpha)\tilde{w}_t + \alpha\tilde{R}_t^k \tag{34}$$

$$\tilde{w}_t - \tilde{R}_t^k = \tilde{u}_t + \tilde{k}_{t-1} - \tilde{l}_t - z_t^z \tag{35}$$

$$\tilde{y}_t = (1+\lambda^p)\left\{(1-\alpha)\tilde{l}_t + \alpha\left(\tilde{u}_t + \tilde{k}_{t-1} - z_t^z\right)\right\} \tag{36}$$

$$\tilde{\pi}_t = \frac{\gamma_p}{1+\beta z^{1-\sigma}\gamma_p}\tilde{\pi}_{t-1} + \frac{\beta z^{1-\sigma}}{1+\beta z^{1-\sigma}\gamma_p}\tilde{\pi}_{t+1} + \frac{1}{\varphi_p\lambda^p\left(1+\beta z^{1-\sigma}\gamma_p\right)}\tilde{mc}_t + z_t^p \tag{37}$$

$$\tilde{R}_t^n = \psi_r\tilde{R}_{t-1}^n + \varepsilon_t^r \tag{38}$$

where $z_t^w := \frac{1}{\varphi_w(1+\lambda^w)}\tilde{\lambda}_t^w$ and $z_t^p := \frac{1}{\varphi_p(1+\lambda^p)(1+\beta z^{1-\sigma}\gamma_p)}\tilde{\lambda}_t^p$ are the reduced-form wage-markup and price-markup shocks, respectively, the variables with $\tilde{}$ denote percentage deviations from their

(detrended) steady-state values, and the variables without time subscripts represent their steady-state values.

3.2.2 Diagnostic expectations

We incorporate DE into the medium-scale DSGE model and rewrite the equilibrium conditions in terms of the RE operator, augmented by the BE parameter θ. Specifically, for arbitrary variables x_t and y_{t+1}, the RE representation of DE is given by

$$\mathbb{E}_t^{DE}[x_t + y_{t+1}] = \mathbb{E}_t[x_t + y_{t+1}] + \theta\left(\mathbb{E}_t[x_t + y_{t+1}] - \mathbb{E}_{t-j}[x_t + y_{t+1}]\right),$$

where θ measures the degree of diagnosticity, and the case $\theta = 0$ coincides with RE. The integer j determines how many periods in the past agents use as a reference for expectation revision. In what follows, we set $j = 1$.

Under DE, the log-linearized equilibrium conditions (26), (27), (28), (30), (31), and (37) from the RE model are replaced with:

$$\left(1 - \frac{\beta\gamma}{z^\sigma}\right)\tilde{\lambda}_t = -\frac{\sigma z}{z-\gamma}\left\{\tilde{c}_t - \frac{\gamma}{z}\left(\tilde{c}_{t-1} - z_t^z\right)\right\} + z_t^b - \frac{\beta\gamma\sigma}{z^\sigma}z_t^z$$
$$+\frac{\beta\gamma}{z^\sigma}\left\{\frac{\sigma z}{z-\gamma}\left((1+\theta)\mathbb{E}_t\tilde{c}_{t+1} - \theta\mathbb{E}_{t-1}\tilde{c}_{t+1} + (1+\theta)\mathbb{E}_t z_{t+1}^z - \theta\mathbb{E}_{t-1}z_{t+1}^z - \frac{\gamma}{z}\left((1+\theta)\tilde{c}_t - \theta\mathbb{E}_{t-1}\tilde{c}_t\right)\right)\right\}$$
$$+\frac{\beta\gamma}{z^\sigma}\left\{\sigma\left((1+\theta)z_t^z - \theta\mathbb{E}_{t-1}z_t^z\right) - (1+\theta)\mathbb{E}_t z_{t+1}^b + \theta\mathbb{E}_{t-1}z_{t+1}^b\right\}$$

$$\tilde{\lambda}_t = (1+\theta)\mathbb{E}_t\tilde{\lambda}_{t+1} - \theta\mathbb{E}_{t-1}\tilde{\lambda}_{t+1} - \sigma(1+\theta)\mathbb{E}_t z_{t+1}^z + \sigma\theta\mathbb{E}_{t-1}z_{t+1}^z - \sigma(1+\theta)z_t^z + \sigma\theta\mathbb{E}_{t-1}z_t^z$$
$$-(1+\theta)\mathbb{E}_t\tilde{\pi}_{t+1} + \theta\mathbb{E}_{t-1}\tilde{\pi}_{t+1} - (1+\theta)\tilde{\pi}_t + \theta\mathbb{E}_{t-1}\tilde{\pi}_t + \tilde{R}_t^n + \tilde{\pi}_t + \sigma z_t^z$$

$$\tilde{\pi}_t + \tilde{w}_t - \tilde{w}_{t-1} + z_t^z = \beta z^{1-\sigma}\left\{(1+\theta)\mathbb{E}_t\tilde{\pi}_{t+1} - \theta\mathbb{E}_{t-1}\tilde{\pi}_{t+1} + (1+\theta)\mathbb{E}_t\tilde{w}_{t+1} - \theta\mathbb{E}_{t-1}\tilde{w}_{t+1}\right\}$$
$$+\beta z^{1-\sigma}\left\{-(1+\theta)\tilde{w}_t + \theta\mathbb{E}_{t-1}\tilde{w}_t + (1+\theta)\mathbb{E}_t z_{t+1}^z - \theta\mathbb{E}_{t-1}z_{t+1}^z\right\} + \frac{1}{\varphi_w\lambda^w}\left(\chi\tilde{l}_t - \tilde{\lambda}_t - \tilde{w}_t + z_t^b\right) + z_t^w$$

$$\varphi_i\left(\tilde{\imath}_t - \tilde{\imath}_{t-1} + z_t^z\right) = \tilde{q}_t + \beta z^{1-\sigma}\varphi_i\left\{(1+\theta)\mathbb{E}_t\tilde{\imath}_{t+1} - \theta\mathbb{E}_{t-1}\tilde{\imath}_{t+1} - (1+\theta)\tilde{\imath}_t + \theta\mathbb{E}_{t-1}\tilde{\imath}_t\right\}$$
$$+\beta z^{1-\sigma}\varphi_i\left\{(1+\theta)\mathbb{E}_t z_{t+1}^z - \theta\mathbb{E}_{t-1}z_{t+1}^z\right\} + z_t^i$$

$$\tilde{q}_t = -\tilde{\lambda}_t + \sigma z_t^z + (1+\theta)\mathbb{E}_t\tilde{\lambda}_{t+1} - \theta\mathbb{E}_{t-1}\tilde{\lambda}_{t+1} - \sigma(1+\theta)\mathbb{E}_t z_{t+1}^z + \sigma\theta\mathbb{E}_{t-1}z_{t+1}^z$$
$$-\sigma(1+\theta)z_t^z + \sigma\theta\mathbb{E}_{t-1}z_t^z + \frac{\beta}{z^\sigma}R^k(1+\theta)\mathbb{E}_t\tilde{R}_{t+1}^k - \frac{\beta}{z^\sigma}R^k\theta\mathbb{E}_{t-1}\tilde{R}_{t+1}^k$$
$$+\frac{\beta}{z^\sigma}(1-\delta)(1+\theta)\mathbb{E}_t\tilde{q}_{t+1} - \frac{\beta}{z^\sigma}(1-\delta)\theta\mathbb{E}_{t-1}\tilde{q}_{t+1}$$

$$\tilde{\pi}_t = \beta z^{1-\sigma}(1+\theta)\mathbb{E}_t\tilde{\pi}_{t+1} - \beta z^{1-\sigma}\theta\mathbb{E}_{t-1}\tilde{\pi}_{t+1} - \beta z^{1-\sigma}\gamma_p(1+\theta)\tilde{\pi}_t + \beta z^{1-\sigma}\gamma_p\theta\mathbb{E}_{t-1}\tilde{\pi}_t$$
$$+\gamma_p\tilde{\pi}_{t-1} + (1+\beta z^{1-\sigma}\gamma_p)z_t^p + \frac{1}{\varphi_p\lambda^p}\tilde{mc}_t$$

The other linearized equations, i.e., (29), (32), (33), (34), (35), (36), and (38), remain unchanged from the RE benchmark.

3.2.3 Cognitive discounting

As in the model under DE, the equilibrium conditions under CD are expressed using the RE operator and the CD parameter ϕ. The RE representation of CD is given by:

$$\mathbb{E}_t^{CD}[x_t + y_{t+1}] = \phi \mathbb{E}_t[x_t + y_{t+1}],$$

where $\phi \in (0, 1]$, with $\phi = 1$ corresponding to the RE limit.

The log-linearized equilibrium conditions (26), (27), (28), (30), (31), and (37) in the RE model are modified as follows:

$$\begin{aligned}
\left(1 - \frac{\beta\gamma}{z^\sigma}\right)\tilde{\lambda}_t = &-\frac{\sigma z}{z-\gamma}\left\{\tilde{c}_t - \frac{\gamma}{z}\left(\tilde{c}_{t-1} - z_t^z\right)\right\} + z_t^b - \frac{\beta\gamma\sigma}{z^\sigma} z_t^z \\
&+ \frac{\beta\gamma}{z^\sigma}\left\{\frac{\sigma z}{z-\gamma}\left(\phi\mathbb{E}_t\tilde{c}_{t+1} + \phi\mathbb{E}_t z_{t+1}^z - \frac{\gamma}{z}\phi\tilde{c}_t\right) + \sigma\phi z_t^z - \phi\mathbb{E}_t z_{t+1}^b\right\} \\
\tilde{\lambda}_t = &\ \phi\mathbb{E}_t\tilde{\lambda}_{t+1} - \sigma\phi\mathbb{E}_t z_{t+1}^z - \sigma\phi z_t^z - \phi\mathbb{E}_t\tilde{\pi}_{t+1} - \phi\tilde{\pi}_t + \tilde{R}_t^n + \tilde{\pi}_t + \sigma z_t^z \\
\tilde{\pi}_t + \tilde{w}_t - \tilde{w}_{t-1} + z_t^z = &\ \beta z^{1-\sigma}\left\{\phi\mathbb{E}_t\tilde{\pi}_{t+1} + \phi\mathbb{E}_t\tilde{w}_{t+1} - \phi\tilde{w}_t + \phi\mathbb{E}_t z_{t+1}^z\right\} \\
&+ \frac{1}{\varphi_w\lambda^w}\left(\chi\tilde{l}_t - \tilde{\lambda}_t - \tilde{w}_t + z_t^b\right) + z_t^w \\
\varphi_i\left(\tilde{\imath}_t - \tilde{\imath}_{t-1} + z_t^z\right) = &\ \tilde{q}_t + \beta z^{1-\sigma}\varphi_i\left(\phi\mathbb{E}_t\tilde{\imath}_{t+1} - \phi\tilde{\imath}_t + \phi\mathbb{E}_t z_{t+1}^z\right) + z_t^i \\
\tilde{q}_t = &-\tilde{\lambda}_t + \sigma z_t^z + \phi\mathbb{E}_t\tilde{\lambda}_{t+1} - \sigma\phi\mathbb{E}_t z_{t+1}^z - \sigma\phi z_t^z + \frac{\beta}{z^\sigma}R^k\phi\mathbb{E}_t\tilde{R}_{t+1}^k + \frac{\beta}{z^\sigma}(1-\delta)\phi\mathbb{E}_t\tilde{q}_{t+1} \\
\tilde{\pi}_t = &\ \beta z^{1-\sigma}\phi\mathbb{E}_t\tilde{\pi}_{t+1} - \beta z^{1-\sigma}\gamma_p\phi\tilde{\pi}_t + \gamma_p\tilde{\pi}_{t-1} + (1 + \beta z^{1-\sigma}\gamma_p)z_t^p + \frac{1}{\varphi_p\lambda^p}\tilde{mc}_t
\end{aligned}$$

The other linearized equations are identical to the RE benchmark.

4 Estimation Strategy

In the model, equilibrium is generally indeterminate under RE and DE because the nominal interest rate follows an AR(1) process and does not satisfy the Taylor principle. In contrast, as shown by Gabaix (2020), the model under CD can exhibit equilibrium determinacy under sufficiently strong degrees of CD even when the Taylor principle fails to hold. Thus, we estimate the model, allowing for both determinacy and indeterminacy, using a full-information Bayesian approach based on the approach of Lubik and Schorfheide (2004). Specifically, the model's likelihood function is constructed not only for the determinacy region of its parameter space but also for the indeterminacy region. While Lubik and Schorfheide (2004) performed model estimation separately for each re-

gion, we estimate the model for both the determinacy and indeterminacy regions simultaneously by adopting a sequential Monte Carlo (SMC) algorithm, as implemented by Hirose et al. (2020, 2023). This algorithm can handle discontinuities in the likelihood function at the boundaries of each region and allows us to recover the entire posterior distribution of the model's parameters.

In this section, we begin by presenting solutions to linear rational expectations models, then explain how Bayesian inference over both the determinacy and indeterminacy regions of the model parameter space is conducted using the SMC algorithm, and finally describe the data and prior distributions used in the model estimation.

4.1 Rational expectations solutions under indeterminacy

Lubik and Schorfheide (2003) derive a full set of solutions to models under indeterminacy of the form

$$\mathbf{s}_t = \mathbf{\Phi}_1^I(\boldsymbol{\theta})\,\mathbf{s}_{t-1} + \mathbf{\Phi}_\varepsilon^I(\boldsymbol{\theta}, \tilde{\mathbf{M}})\,\boldsymbol{\varepsilon}_t + \mathbf{\Phi}_\zeta^I(\boldsymbol{\theta})\,\zeta_t, \tag{39}$$

where $\mathbf{\Phi}_1^I(\boldsymbol{\theta})$, $\mathbf{\Phi}_\varepsilon^I(\boldsymbol{\theta}, \tilde{\mathbf{M}})$, and $\mathbf{\Phi}_\zeta^I(\boldsymbol{\theta})$ are coefficient matrices that depend on the vector $\boldsymbol{\theta}$ of model parameters and an arbitrary matrix $\tilde{\mathbf{M}}$; $\mathbf{s}_t$ is a vector of endogenous variables; $\boldsymbol{\varepsilon}_t$ is a vector of fundamental shocks; and $\zeta_t \sim$ i.i.d. $N(0, \sigma_\zeta^2)$ is a reduced-form sunspot shock.[11] A nonzero $\tilde{\mathbf{M}}$ implies that the contributions of fundamental shocks to forecast errors are correlated with those of sunspot shocks. The indeterminacy solution (39) exhibits three characteristics. First, the equilibrium dynamics are driven not only by the fundamental shocks $\boldsymbol{\varepsilon}_t$ but also by the sunspot shock ζ_t. Second, the solution is not unique due to the presence of the arbitrary matrix $\tilde{\mathbf{M}}$. Third, $\mathbf{\Phi}_1^I(\boldsymbol{\theta})$ in the solution induces more persistent dynamics than its counterpart $\mathbf{\Phi}_1^D(\boldsymbol{\theta})$ in the determinacy solution presented below, because fewer autoregressive roots (*i.e.*, eigenvalues) in $\mathbf{\Phi}_1^I(\boldsymbol{\theta})$ are suppressed to zero.[12]

In the case of determinacy, the solution reduces to

$$\mathbf{s}_t = \mathbf{\Phi}_1^D(\boldsymbol{\theta})\,\mathbf{s}_{t-1} + \mathbf{\Phi}_\varepsilon^D(\boldsymbol{\theta})\,\boldsymbol{\varepsilon}_t, \tag{40}$$

where $\mathbf{\Phi}_1^D(\boldsymbol{\theta})$ and $\mathbf{\Phi}_\varepsilon^D(\boldsymbol{\theta})$ depend only on the model parameters $\boldsymbol{\theta}$. Thus, the solution is uniquely determined and driven only by the fundamental shocks $\boldsymbol{\varepsilon}_t$.

Under indeterminacy, $\tilde{\mathbf{M}}$ is estimated jointly with the other model parameters to characterize the law of motion for $\mathbf{s}_t$. Following Lubik and Schorfheide (2004), we assume $\tilde{\mathbf{M}}$ is distributed around a specific $\mathbf{M}^*(\boldsymbol{\theta})$, derived from a particular solution, and write $\tilde{\mathbf{M}} = \mathbf{M}^*(\boldsymbol{\theta}) + \mathbf{M}$. The components of $\mathbf{M}$, which capture correlations between fundamental and sunspot shocks, are estimated with prior means set to zero. As proposed by Lubik and Schorfheide (2004), $\mathbf{M}^*(\boldsymbol{\theta})$ is

[11] Instead of the term $\mathbf{\Phi}_\zeta^I(\boldsymbol{\theta})\,\zeta_t$ in the indeterminacy solution (39), Lubik and Schorfheide (2003) originally consider $\mathbf{\Phi}_\zeta^I(\boldsymbol{\theta}, \mathbf{M}_\zeta)\,\boldsymbol{\zeta}_t$, where $\mathbf{M}_\zeta$ is an arbitrary matrix and $\boldsymbol{\zeta}_t$ is a vector of sunspot shocks. For identification, however, Lubik and Schorfheide (2004) impose a normalization on $\mathbf{M}_\zeta$ with the dimension of the sunspot shock vector set to unity. Such a normalized shock is referred to as a "reduced-form sunspot shock" because it contains beliefs associated with all the expectational variables.

[12] For details, see Lubik and Schorfheide (2003, 2004).

selected such that the contemporaneous impulse responses of the endogenous variables to the fundamental shocks (*i.e.*, $\partial \mathbf{s}_t / \partial \boldsymbol{\varepsilon}_t$) remain continuous at the boundary between the determinacy and indeterminacy regions of the model parameter space, referred to as a "continuity solution." More specifically, for each set of $\boldsymbol{\theta}$, the procedure searches for a vector $\boldsymbol{\theta}^*$ that lies on the boundary of the determinacy region, and selects $\mathbf{M}^*(\boldsymbol{\theta})$ to minimize the discrepancy between $\partial \mathbf{s}_t / \partial \boldsymbol{\varepsilon}_t(\boldsymbol{\theta}, \mathbf{M}^*(\boldsymbol{\theta}))$, and $\partial \mathbf{s}_t / \partial \boldsymbol{\varepsilon}_t(\boldsymbol{\theta}^*)$, using a least-squares criterion. To find $\boldsymbol{\theta}^*$, the procedure replaces the exogenous process for the nominal interest rate (25) with a simple inflation-targeting rule of the form:

$$\tilde{R}_t^n = \psi_r \tilde{R}_{t-1}^n + (1 - \psi_r)\psi_\pi \tilde{\pi}_t + \varepsilon_t^r,$$

and gradually increases the parameter value of ψ_π—holding the other parameters in $\boldsymbol{\theta}$ fixed—until the equilibrium becomes determinate.

4.2 Bayesian inference

To conduct Bayesian inference over both the determinacy and indeterminacy regions of the model parameter space, we construct the likelihood function for a sample of observations $\mathbf{Y}^T = [\mathbf{Y}_1, \ldots, \mathbf{Y}_T]'$ as

$$p(\mathbf{Y}^T|\boldsymbol{\theta}, \mathbf{M}) = \mathbf{1}\{\boldsymbol{\theta} \in \boldsymbol{\Theta}^D\}\, p^D(\mathbf{Y}^T|\boldsymbol{\theta}) + \mathbf{1}\{\boldsymbol{\theta} \in \boldsymbol{\Theta}^I\}\, p^I(\mathbf{Y}^T|\boldsymbol{\theta}, \mathbf{M}),$$

where $\boldsymbol{\Theta}^D$ and $\boldsymbol{\Theta}^I$ denote the determinacy and indeterminacy regions; $\mathbf{1}\{\boldsymbol{\theta} \in \boldsymbol{\Theta}^i\}$, $i \in \{D, I\}$ is an indicator function that equals one if $\boldsymbol{\theta} \in \boldsymbol{\Theta}^i$ and zero otherwise; and $p^D(\mathbf{Y}^T|\boldsymbol{\theta})$ and $p^I(\mathbf{Y}^T|\boldsymbol{\theta}, \mathbf{M})$ are the likelihood functions of the state-space models, consisting of observation equations and either the determinacy solution (40) or the indeterminacy solution (39). Then, by Bayes' theorem, updating the prior distribution $p(\boldsymbol{\theta}, \mathbf{M})$ with the sample observations $\mathbf{Y}^T$ leads to the posterior distribution

$$p(\boldsymbol{\theta}, \mathbf{M}|\mathbf{Y}^T) = \frac{p(\mathbf{Y}^T|\boldsymbol{\theta}, \mathbf{M})p(\boldsymbol{\theta}, \mathbf{M})}{p(\mathbf{Y}^T)} = \frac{p(\mathbf{Y}^T|\boldsymbol{\theta}, \mathbf{M})p(\boldsymbol{\theta}, \mathbf{M})}{\int p(\mathbf{Y}^T|\boldsymbol{\theta}, \mathbf{M})p(\boldsymbol{\theta}, \mathbf{M})d\boldsymbol{\theta}d\mathbf{M}}.$$

To approximate the posterior distribution, we adopt a generic SMC algorithm with likelihood tempering, as described in Herbst and Schorfheide (2014, 2015). The details of the algorithm are provided in Appendix C. Based on the particle population from the final importance sampling step, we make inferences about the parameters and approximate the marginal data densities.

4.3 Data and prior distributions

The data used for model estimation consist of seven quarterly time series for the Japanese economy: the log differences of real GDP, real consumption, real investment, real wage, and the GDP deflator; the log of hours worked; and the overnight call rate. Real GDP, real consumption, and real investment are measured on a per capita basis, using the population aged 15 and over. Real consumption and investment are calculated by dividing nominal private consumption expenditure and gross private domestic investment expenditure, respectively, by the GDP deflator. The series

for real wage and hours worked are constructed following Sugo and Ueda (2008), with the hours worked series demeaned prior to estimation.

The data are related to model-implied variables by the following measurement equations:

$$\begin{bmatrix} 100\Delta \log Y_t \\ 100\Delta \log C_t \\ 100\Delta \log I_t \\ 100\Delta \log W_t \\ 100 \log l_t \\ 100\Delta \log P_t \\ 100 \log R_t^n \end{bmatrix} = \begin{bmatrix} \bar{z} \\ \bar{z} \\ \bar{z} \\ \bar{z} \\ \bar{l} \\ \bar{\pi} \\ \bar{r} + \bar{\pi} \end{bmatrix} + \begin{bmatrix} \tilde{y}_t - \tilde{y}_{t-1} + z_t^z \\ \tilde{c}_t - \tilde{c}_{t-1} + z_t^z \\ \tilde{\imath}_t - \tilde{\imath}_{t-1} + z_t^z \\ \tilde{w}_t - \tilde{w}_{t-1} + z_t^z \\ \tilde{l}_t \\ \tilde{\pi}_t \\ \tilde{R}_t^n \end{bmatrix},$$

where $\bar{z} = 100 \log z$, $\bar{l} = 100 \log l$, $\bar{\pi} = 100 \log \pi$, and $\bar{r} = 100 \log R$.

The sample period is from 1999Q1 to 2024Q1, when the Bank of Japan conducted the virtually zero interest rate policy, with the exception of August 2000–March 2001 and July 2006–December 2008.

Before estimation, some parameters are fixed to avoid identification issues. The subjective discount factor is fixed at $\beta = 0.999$. Following Sugo and Ueda (2008), we set the steady-state depreciation rate at $\delta = 0.06/4$, the capital elasticity of output at $\alpha = 0.37$, and the steady-state wage markup at $\lambda^w = 0.2$. The steady-state ratio of external demand to output is set at the sample mean; *i.e.*, $d/y = 0.247$.

All other parameters in the model are estimated, and their prior distributions are presented in Table 1. For the degree of DE (θ), we assign the normal distribution with a mean of unity and a standard deviation of 0.3, following L'Huillier et al. (2024), who estimate the same parameter in a medium-scale New Keynesian model for the US economy. Regarding the parameter on CD (ϕ), we impose the beta distribution with a mean of 0.85 and a standard deviation of 0.05, as in Hirose et al. (2024), who estimate a nonlinear New Keynesian model with the zero lower bound on the nominal interest rate under CD.

Most of the priors for the structural parameters $(\sigma, \gamma, \chi, \mu, \varphi_i, \lambda^p, \gamma_p, \psi_r)$ are taken from Hirose (2020), who estimate a similar model to ours for Japan's economy. The parameters on wage and price adjustment costs (φ_w, φ_p) are centered around 20 and 30, respectively, following Iwasaki et al. (2021), who estimate these parameters in a nonlinear New Keynesian model with downward nominal rigidity for advanced economies, including Japan.

The priors for the steady-state values for the balanced growth rate, the hours worked, the inflation rate, and the real interest rate $(\bar{z}, \bar{l}, \bar{\pi}, \bar{r})$ are set using a normal distribution with a mean based on the sample average of the corresponding data.

The priors for the shock persistence parameters (ρ_x, $x \in \{z, b, i, d, w, p\}$) are set using the beta distribution with a mean of 0.5 and a standard deviation of 0.15. For the standard deviations of the shock innovations (σ_x, $x \in \{z, b, i, d, w, p, r, s\}$), we set $\nu = 0.15$ and $s = 4$ in the inverse gamma distribution of the form $p(\sigma|\nu, s) \propto \sigma^{-\nu-1} e^{-\nu s^2/2\sigma^2}$. For the components $M_x, x \in \{z, b, i, d, w, p, r\}$

Table 1: Prior Distributions of Parameters

Parameter		Distribution	Mean	S.D.
θ	Degree of diagnosticity	Normal	1.000	0.300
ϕ	Degree of cognitive discounting	Beta	0.850	0.050
$\overline{z}$	Steady-state output growth rate	Gamma	0.129	0.050
$\overline{\pi}$	Steady-state inflation rate	Normal	-0.039	0.050
$\bar{l}$	Steady-state hours worked	Normal	0.000	0.050
σ	Relative risk aversion	Gamma	1.500	0.100
γ	Habit persistence	Beta	0.500	0.100
φ_w	Wage adjustment cost	Gamma	20.00	5.000
χ	Inverse elasticity of labor supply	Gamma	2.000	0.750
μ	Capital utilization adjustment cost	Gamma	1.000	0.500
φ_i	Investment adjustment cost	Gamma	4.000	1.000
λ_p	Steady-state price markup	Gamma	0.150	0.050
φ_p	Investment adjustment cost	Gamma	30.00	5.000
γ_p	Price indexation	Beta	0.500	0.150
ψ_r	Interest rate smoothing	Beta	0.750	0.150
ρ_z	Persistence of technology shock	Beta	0.500	0.150
ρ_b	Persistence of preference shock	Beta	0.500	0.150
ρ_i	Persistence of investment shock	Beta	0.500	0.150
ρ_d	Persistence of external demand shock	Beta	0.500	0.150
ρ_w	Persistence of wage markup shock	Beta	0.500	0.150
ρ_p	Persistence of price markup shock	Beta	0.500	0.150
σ_z	Standard deviation of technology shock	Inverse gamma	0.500	4.000
σ_b	Standard deviation of preference shock	Inverse gamma	0.500	4.000
σ_i	Standard deviation of investment shock	Inverse gamma	0.500	4.000
σ_d	Standard deviation of external demand shock	Inverse gamma	0.500	4.000
σ_w	Standard deviation of wage markup shock	Inverse gamma	0.500	4.000
σ_p	Standard deviation of price markup shock	Inverse gamma	0.500	4.000
σ_r	Standard deviation of monetary policy shock	Inverse gamma	0.500	4.000
σ_s	Standard deviation of sunspot shock	Inverse gamma	0.500	4.000
M_z	Arbitrary parameter on technology shock	Normal	0.000	1.000
M_b	Arbitrary parameter on preference shock	Normal	0.000	1.000
M_i	Arbitrary parameter on investment shock	Normal	0.000	1.000
M_d	Arbitrary parameter on external demand shock	Normal	0.000	1.000
M_w	Arbitrary parameter on wage markup shock	Normal	0.000	1.000
M_p	Arbitrary parameter on price markup shock	Normal	0.000	1.000
M_r	Arbitrary parameter on monetary policy shock	Normal	0.000	1.000

Notes: The prior probability of equilibrium determinacy is 0.000 under the RE and DE, 0.160 under the CD, and 0.460 under the CD with CD forecast errors. Inverse gamma distributions are of the form $p(\sigma|\nu, s) \propto \sigma^{-\nu-1}e^{-\nu s^2/2\sigma^2}$, where ν and s are respectively set at the mean and standard deviation (S.D.) values in the table.

of the arbitrary matrix $\mathbf{M}$ in the indeterminacy solution, we assign the standard normal distribution, following Lubik and Schorfheide (2004).

5 Empirical Results and Evaluation

5.1 Posterior estimates of parameters and model selection

Table 2 presents the posterior estimates of the model parameters and the log marginal data densities across five specifications of expectation formation and forecast errors: RE, DE with RE forecast errors, DE with DE forecast errors, CD with RE forecast errors, and CD with CD forecast errors.

Our primary interest is in the estimates of the degrees of DE (θ) and CD (ϕ). The posterior mean of θ is estimated to be 1.228 with the 90% credible interval of $[0.953, 1.489]$ under RE forecast errors, far from the RE limit of 0, which is consistent with the existing literature.[13] In contrast, θ is estimated to be 0.045 under DE forecast errors—close to zero—suggesting that the model with DE forecast errors does not require a significant degree of DE to match the data. This is mainly because the DE forecast error specification includes more state variables than its RE counterpart, enabling it to generate highly persistent dynamics, as shown in Section 2.1.2.[14] If the model exhibited strong diagnosticity, the resulting excessive persistence of endogenous variables would be inconsistent with the data. Consequently, the model with DE forecast errors is estimated with only a limited degree of DE.

The posterior mean of ϕ is estimated at 0.911 with CD forecast errors, indicating a substantial degree of behavioral distortion. In contrast, under RE forecast errors, ϕ is estimated at 0.976, much closer to the RE limit of 1. As discussed in Section 2.3, equilibrium dynamics under CD with CD forecast errors closely resemble those under RE. In other words, CD forecast errors dampen the effect of CD, requiring a stronger degree of CD to match the model to the data. On the contrary, even a small degree of distortion on CD leads to a much large deviation from the RE benchmark under RE forecast errors, allowing the model to match the data with a much weaker degree of CD, as reflected in the higher estimated value of $\phi = 0.976$.

To compare the empirical performance across the different specifications, the last rows in Table 2 show the log marginal data densities of the estimated models. The model combining DE with RE forecast errors yields the highest marginal data density (-805.719), followed by the CD model with CD forecast errors (-852.880). Both outperform the benchmark RE model (-876.519). In contrast, the DE model with DE forecast errors and the CD model with RE forecast errors produce lower marginal data densities compared to their RE-based counterparts. The differences in log marginal data densities thus provide evidence in favor of the DE model with RE forecast errors.

To better understand this ranking of the models' empirical performance, we examine the auto-correlation functions of observed variables used in estimation, including the growth rates of output,

[13] The diagnosticity parameter θ is estimated to be within 0.5 and 2 in the literature. See, for example, Bordalo et al. (2019), D'Arienzo (2020), Pflueger et al. (2020), Bordalo et al. (2021), Bianchi et al. (2024a), L'Huillier et al. (2024), Na and Yoo (2025).

[14] Compare the solution under indeterminacy with RE forecast errors (12) and with DE forecast errors (15).

Table 2: Posterior Estimates of Parameters

	RE		DE+RE forecast errors		DE+DE forecast errors	
Parameter	Mean	90% interval	Mean	90% interval	Mean	90% interval
θ	-	-	1.228	[0.953, 1.489]	0.045	[-0.032, 0.135]
$\overline{z}$	0.174	[0.090, 0.265]	0.086	[0.039, 0.130]	0.115	[0.064, 0.164]
$\overline{\pi}$	0.008	[-0.062, 0.086]	-0.091	[-0.147, -0.031]	-0.101	[-0.195, -0.003]
$\bar{l}$	-0.047	[-0.105, 0.015]	0.011	[-0.063, 0.083]	0.022	[-0.079, 0.109]
σ	1.384	[1.238, 1.527]	1.339	[1.193, 1.477]	1.422	[1.268, 1.560]
γ	0.184	[0.120, 0.248]	0.435	[0.363, 0.511]	0.229	[0.157, 0.298]
φ_w	28.464	[19.309, 36.817]	26.512	[20.358, 33.122]	33.487	[26.681, 39.657]
χ	1.645	[0.761, 2.467]	2.265	[1.256, 3.246]	0.997	[0.491, 1.494]
μ	1.752	[1.098, 2.481]	1.344	[0.603, 2.033]	0.127	[0.025, 0.212]
φ_i	3.262	[2.306, 4.228]	4.342	[3.053, 5.558]	1.888	[1.330, 2.428]
λ_p	0.221	[0.149, 0.293]	0.227	[0.157, 0.303]	0.236	[0.165, 0.315]
φ_p	29.803	[22.898, 36.238]	32.819	[24.931, 39.344]	33.285	[25.986, 40.304]
γ_p	0.471	[0.215, 0.721]	0.375	[0.198, 0.578]	0.681	[0.483, 0.883]
ψ_r	0.803	[0.694, 0.933]	0.814	[0.732, 0.896]	0.888	[0.813, 0.961]
ρ_z	0.200	[0.103, 0.295]	0.139	[0.053, 0.218]	0.121	[0.035, 0.199]
ρ_b	0.476	[0.221, 0.729]	0.699	[0.467, 0.924]	0.871	[0.818, 0.921]
ρ_i	0.874	[0.784, 0.979]	0.908	[0.867, 0.958]	0.367	[0.151, 0.579]
ρ_d	0.862	[0.798, 0.923]	0.845	[0.784, 0.905]	0.836	[0.774, 0.896]
ρ_w	0.578	[0.443, 0.712]	0.587	[0.413, 0.735]	0.461	[0.325, 0.608]
ρ_p	0.647	[0.495, 0.820]	0.653	[0.501, 0.807]	0.362	[0.190, 0.546]
σ_z	1.932	[1.696, 2.143]	1.589	[1.272, 1.919]	2.351	[2.115, 2.578]
σ_b	0.595	[0.293, 0.901]	0.699	[0.322, 1.057]	2.373	[1.905, 2.797]
σ_i	2.934	[2.178, 3.713]	1.896	[1.546, 2.198]	0.569	[0.294, 0.842]
σ_d	2.892	[2.643, 3.163]	3.123	[2.794, 3.440]	2.581	[2.354, 2.819]
σ_w	1.219	[0.966, 1.447]	1.230	[0.904, 1.547]	1.116	[0.949, 1.273]
σ_p	0.416	[0.338, 0.482]	0.352	[0.260, 0.433]	0.521	[0.415, 0.617]
σ_r	0.098	[0.087, 0.109]	0.102	[0.091, 0.113]	0.097	[0.084, 0.110]
σ_s	0.543	[0.425, 0.678]	0.533	[0.380, 0.680]	0.735	[0.496, 0.970]
M_z	-0.623	[-0.841, -0.420]	-1.445	[-1.798, -1.067]	-0.773	[-0.957, -0.566]
M_b	-0.410	[-0.873, 0.023]	-0.322	[-0.857, 0.327]	-0.601	[-0.725, -0.480]
M_i	-0.107	[-0.177, -0.028]	-0.228	[-0.330, -0.120]	0.314	[-0.525, 1.295]
M_d	-0.134	[-0.180, -0.089]	-0.222	[-0.276, -0.165]	-0.107	[-0.176, -0.043]
M_w	-0.606	[-0.765, -0.437]	-0.548	[-0.706, -0.369]	-0.909	[-1.156, -0.665]
M_p	-0.074	[-0.369, 0.232]	0.916	[0.405, 1.468]	-0.830	[-1.316, -0.319]
M_r	0.162	[-1.333, 1.908]	0.199	[-1.267, 1.560]	-0.146	[-1.630, 1.487]
$\log p(\mathbf{Y}^T)$	-876.519		-805.719		-967.915	

Table 2: Posterior Estimates of Parameters (Continued)

	CD+RE forecast errors		CD+CD forecast errors	
Parameter	Mean	90% interval	Mean	90% interval
ϕ	0.976	[0.953, 0.996]	0.911	[0.891, 0.935]
$\overline{z}$	0.085	[0.029, 0.144]	0.089	[0.047, 0.131]
$\overline{\pi}$	-0.019	[-0.094, 0.067]	-0.120	[-0.174, -0.063]
$\bar{l}$	0.022	[-0.052, 0.090]	0.015	[-0.055, 0.090]
σ	1.323	[1.172, 1.466]	1.317	[1.165, 1.476]
γ	0.234	[0.136, 0.319]	0.152	[0.091, 0.207]
φ_w	32.005	[23.644, 39.575]	27.964	[20.005, 36.365]
χ	1.696	[1.038, 2.373]	0.592	[0.227, 0.978]
μ	1.745	[1.260, 2.297]	3.432	[2.299, 4.348]
φ_i	2.226	[1.640, 2.737]	3.858	[3.230, 4.526]
λ_p	0.170	[0.105, 0.237]	0.294	[0.218, 0.376]
φ_p	30.363	[24.237, 36.095]	33.644	[27.518, 39.732]
γ_p	0.502	[0.274, 0.734]	0.655	[0.467, 0.876]
ψ_r	0.889	[0.820, 0.957]	0.817	[0.686, 0.940]
ρ_z	0.183	[0.094, 0.283]	0.158	[0.057, 0.252]
ρ_b	0.590	[0.318, 0.908]	0.375	[0.180, 0.564]
ρ_i	0.792	[0.698, 0.894]	0.754	[0.656, 0.847]
ρ_d	0.825	[0.758, 0.894]	0.837	[0.776, 0.910]
ρ_w	0.480	[0.324, 0.636]	0.475	[0.337, 0.623]
ρ_p	0.588	[0.426, 0.755]	0.384	[0.223, 0.542]
σ_z	1.984	[1.734, 2.222]	1.764	[1.405, 2.137]
σ_b	1.370	[0.692, 2.023]	0.459	[0.254, 0.691]
σ_i	2.703	[2.059, 3.345]	3.374	[2.681, 4.041]
σ_d	2.587	[2.344, 2.794]	2.630	[2.295, 2.994]
σ_w	1.134	[0.940, 1.324]	1.142	[0.950, 1.337]
σ_p	0.508	[0.402, 0.602]	0.430	[0.367, 0.493]
σ_r	0.098	[0.083, 0.111]	0.101	[0.089, 0.112]
σ_s	0.518	[0.359, 0.670]	0.625	[0.462, 0.803]
M_z	-0.562	[-0.790, -0.339]	-0.600	[-0.804, -0.403]
M_b	-0.285	[-0.413, -0.158]	0.319	[-0.474, 1.094]
M_i	-0.202	[-0.325, -0.081]	0.252	[0.144, 0.353]
M_d	-0.133	[-0.193, -0.076]	-0.099	[-0.150, -0.051]
M_w	-0.542	[-0.675, -0.385]	-0.926	[-1.206, -0.657]
M_p	-0.213	[-0.639, 0.232]	-0.649	[-0.996, -0.302]
M_r	0.540	[-0.922, 2.001]	0.128	[-1.360, 1.407]
$\log p(\mathbf{Y}^T)$	-915.986		-852.880	

Notes: This table reports the posterior mean and 90 percent highest posterior density intervals based on $10,000$ particles from the final importance sampling in the SMC algorithm. In the table, $\log p(\mathbf{Y}^T)$ represents the SMC-based approximation of log marginal data density.

Figure 2: Autocorrelation Functions

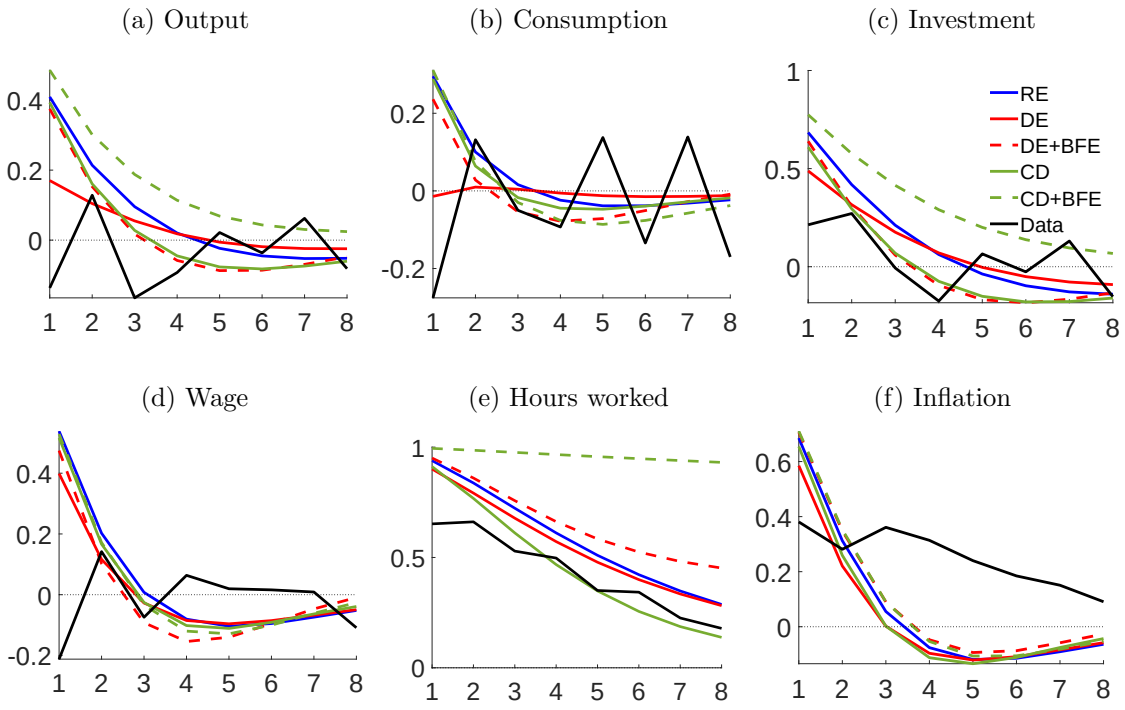

Notes: This figure compares the autocorrelation functions of the growth rates of output, consumption, investment, and wage; the level of hours worked; and the inflation rate across the estimated models, as functions of the lags shown on the horizontal axes. The models include the RE model (blue lines), the DE model with RE forecast errors (solid red lines), the DE model with DE forecast errors (dashed red lines), the CD model with RE forecast errors (solid green lines), and the CD model with CD forecast errors (dashed green lines). The results, based on the posterior mean estimates of the parameters, are compared with those from the data (black lines).

consumption, investment, and wage; the level of hours worked; and the inflation rate. Figure 2 displays these autocorrelation functions across the five estimated models, plotted against the number of lags. The RE model is shown in blue; the DE models with RE and DE forecast errors are shown in solid and dashed red lines, respectively; and the CD models with RE and CD forecast errors are shown in solid and dashed green lines, respectively. The model-implied autocorrelations are computed using the posterior mean estimates of the parameters and are compared with those observed in the data, represented by black lines.

Given that the marginal data densities are evaluated as one-step-ahead pseudo-out-of-sample predictive scores, the autocorrelations at the shortest lag (*i.e.*, the first lag) are most relevant for model selection. From this perspective, the DE model with RE forecast errors exhibits first-lag autocorrelations that are closest to those observed in the data across all six observables. Moreover, this model performs well in replicating the near-zero autocorrelations at longer lags for the growth rates of output, consumption, investment, and wage. The CD model with CD forecast errors ranks second in terms of marginal data densities; however, the autocorrelation functions implied

by this model exhibit excessive persistence relative to the data for the growth rates of output and investment, as well as the level of hours worked. Nevertheless, this strong persistence may enhance one-step-ahead forecast performance and, in turn, lead to a higher marginal data density.

The strong empirical performance of the DE model with RE forecast errors is also reflected in its model-implied covariance matrix. Table 3 compares the squared differences between the model-implied and sample covariance matrices for the seven observed variables used in the estimation: the growth rates of output, consumption, investment, and wage; the level of hours worked; the inflation rate; and the nominal interest rate. The comparison spans the five model specifications considered in this paper. The model-implied covariance matrices are obtained by solving the discrete Lyapunov equation using the posterior mean estimates of the model parameters.

The DE model with RE forecast errors yields the smallest squared differences in nearly all elements of the covariance matrix across the different specifications. Notably, the model perfectly replicates the observed covariances between output and consumption, output and investment, and investment and inflation. The CD model with RE forecast errors also performs well in replicating the observed covariance matrix, although its marginal data density ranks fourth. This discrepancy may arise because the marginal data density reflects the model's one-step-ahead forecast performance rather than the accuracy of its implied covariance matrix. It is also worth noting that the DE model with DE forecast errors and the CD model with CD forecast errors display large squared differences in the variance of hours worked. This result is consistent with the excessive persistence in hours worked implied by these models, as illustrated in Figure 2.

5.2 Impulse Response Functions

To understand the dynamic properties of BE models under indeterminacy, we compare IRFs across different specifications of expectation formation and forecast errors. We focus on IRFs to technology shocks and the sunspot shocks, both of which play significant roles in the variance and historical decompositions discussed in Sections 5.3 and 5.4, respectively. IRFs to the other shocks are presented in Appendix D.

Figure 3 displays the IRFs of the growth rates of output, consumption, investment, and wage, as well as the level of hours worked and the inflation rate, in response to a one-standard-deviation technology shock. The responses are expressed as percentage deviations from steady-state values and are based on the posterior mean parameter estimates for each model: the RE model (blue solid lines), the DE model with RE forecast errors (red solid lines), the DE model with DE forecast errors (red dashed lines), the CD model with RE forecast errors (green solid lines), and the CD model with CD forecast errors (green dashed lines). As discussed in Section 4.1, our equilibrium solution under indeterminacy allows for correlations between fundamental shocks and sunspot shocks. Consequently, the IRFs for each fundamental shock reflect the combined effects of both the fundamental shock and its correlated sunspot shocks.

First, consider how technology shocks propagate in the DE model with RE forecast errors, which exhibits the best fit to the data among other models (see Section 5.1). The technology shock

Table 3: Squared Differences Between the Model-Implied and Sample Covariance Matrices

	$\Delta \log Y_t$	$\Delta \log C_t$	$\Delta \log I_t$	$\Delta \log W_t$	$\log l_t$	$\Delta \log P_t$	$\log R_t^n$
RE model:							
$\Delta \log Y_t$	1.73	0.10	4.77	2.03	0.71	0.26	0.00
$\Delta \log C_t$		0.51	2.14	1.09	0.18	0.38	0.00
$\Delta \log I_t$			44.80	2.91	5.79	0.00	0.00
$\Delta \log W_t$				5.13	0.24	0.72	0.00
$\log l_t$					144.42	0.21	0.00
$\Delta \log P_t$						0.48	0.00
$\log R_t^n$							0.00
DE model:							
$\Delta \log Y_t$	0.08	0.00	0.00	0.85	0.05	0.18	0.00
$\Delta \log C_t$		0.36	2.87	0.62	0.08	0.13	0.00
$\Delta \log I_t$			0.75	0.55	0.29	0.00	0.00
$\Delta \log W_t$				3.05	0.03	0.42	0.00
$\log l_t$					26.04	0.01	0.00
$\Delta \log P_t$						0.26	0.00
$\log R_t^n$							0.00
DE model with DE forecast errors:							
$\Delta \log Y_t$	4.55	0.77	11.68	2.47	4.62	0.29	0.00
$\Delta \log C_t$		0.24	0.16	1.06	0.43	0.18	0.00
$\Delta \log I_t$			44.67	4.73	18.04	0.26	0.00
$\Delta \log W_t$				3.86	3.27	0.58	0.00
$\log l_t$					979.52	2.72	0.02
$\Delta \log P_t$						0.88	0.00
$\log R_t^n$							0.00
CD model:							
$\Delta \log Y_t$	2.17	0.59	4.86	3.01	0.60	0.33	0.00
$\Delta \log C_t$		2.41	2.08	2.47	0.19	0.35	0.00
$\Delta \log I_t$			42.58	3.39	5.09	0.06	0.00
$\Delta \log W_t$				5.90	0.22	0.80	0.00
$\log l_t$					84.25	0.36	0.01
$\Delta \log P_t$						0.65	0.00
$\log R_t^n$							0.00
CD model with CD forecast errors:							
$\Delta \log Y_t$	4.46	0.69	20.52	3.00	2.77	0.08	0.00
$\Delta \log C_t$		1.59	0.00	1.34	0.40	0.81	0.00
$\Delta \log I_t$			138.73	9.45	25.29	0.80	0.00
$\Delta \log W_t$				7.16	0.87	0.84	0.00
$\log l_t$					11890.24	1.79	0.01
$\Delta \log P_t$						0.99	0.00
$\log R_t^n$							0.00

Notes: This table compares the squared differences between the model-implied and sample covariance matrices for the growth rates of output, consumption, investment, and wage; the level of hours worked; and the inflation rate across the estimated models: the RE model, the DE model (with RE forecast errors), the DE model with DE forecast errors, the CD model (with RE forecast errors), and the CD model with CD forecast errors. The model-implied covariance matrices are computed by solving the discrete Lyapunov equation, given the posterior mean estimates of the parameters.

Figure 3: Impulse Responses to Technology Shocks

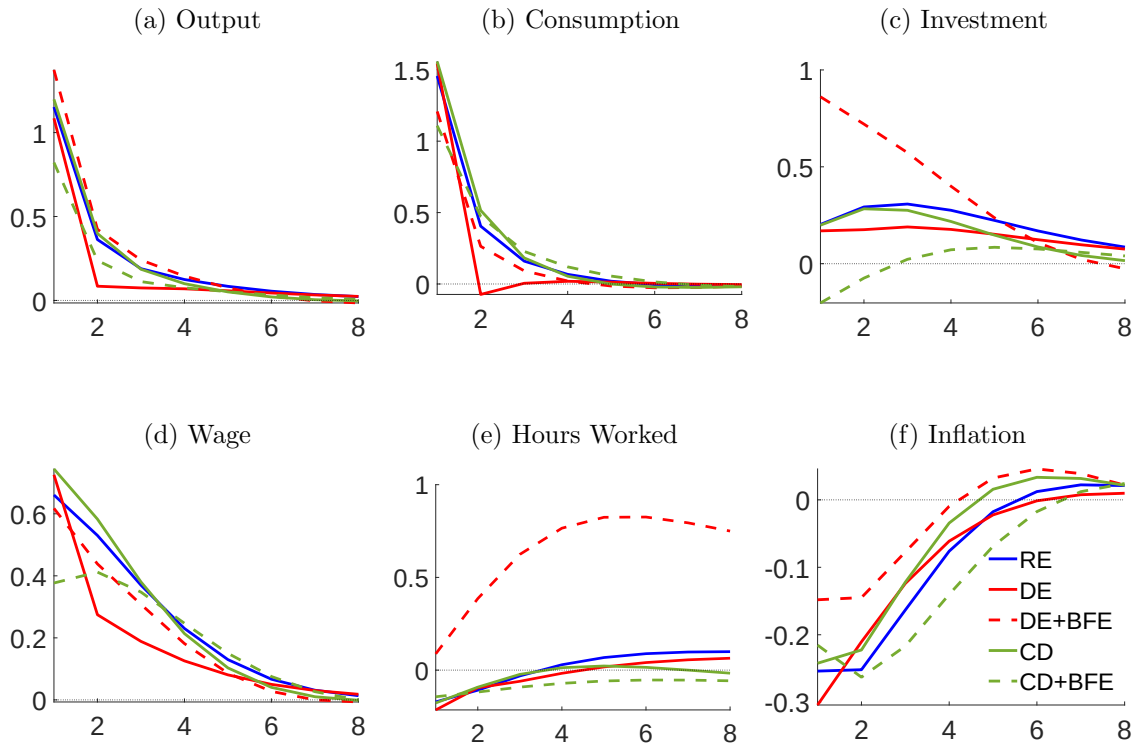

Notes: The panels depict the IRFs for the growth rates of output, consumption, and investment, and wage; the level of hours worked; and the inflation rate to a one-standard-deviation shock to technology. The responses are based on the posterior mean estimates of parameters in each estimated model: the RE model, the DE model with RE forecast errors (DE), the DE model with DE forecast errors (DE+BFE), the CD model with RE forecast errors (CD), and the CD model with CD forecast errors (CD+BFE).

expands production capacity, leading to higher output, consumption, and investment while reducing inflation and hours worked. Under determinacy, it is well known that DE models endogenously generate overreaction and systematic reversals, as documented in Bianchi et al. (2024a), L'Huillier et al. (2024), and Na and Yoo (2025). This feature is also present under indeterminacy. In the DE model with RE forecast errors, output, consumption, and wage exhibit rapid reversals following their initial responses.[15]

It should be noted, however, that the present IRFs are confounded by cross-equation restrictions, as all structural parameters are influenced by behavioral distortions. To isolate the role of behavioral distortion, *i.e.*, diagnosticity, we compare the IRFs in the DE model with RE forecast errors to those from a counterfactual RE scenario (RE counterfactual) that retains the estimated structural parameters but sets the DE parameter $\theta = 0$. Figure 4 presents the IRFs of selected quantities

[15] Appendix D shows that several quantities and prices display (over-)reaction followed by reversals across other shocks: consumption (MEI shock); consumption, investment, and inflation (external demand shock); output, consumption, and investment (wage and price markup shocks); output, consumption, investment, wage, and inflation (monetary policy shock); and output, consumption, investment, and wage (sunspot shock).

Figure 4: Impulse Responses under DE and RE Counterfactual: Quantities

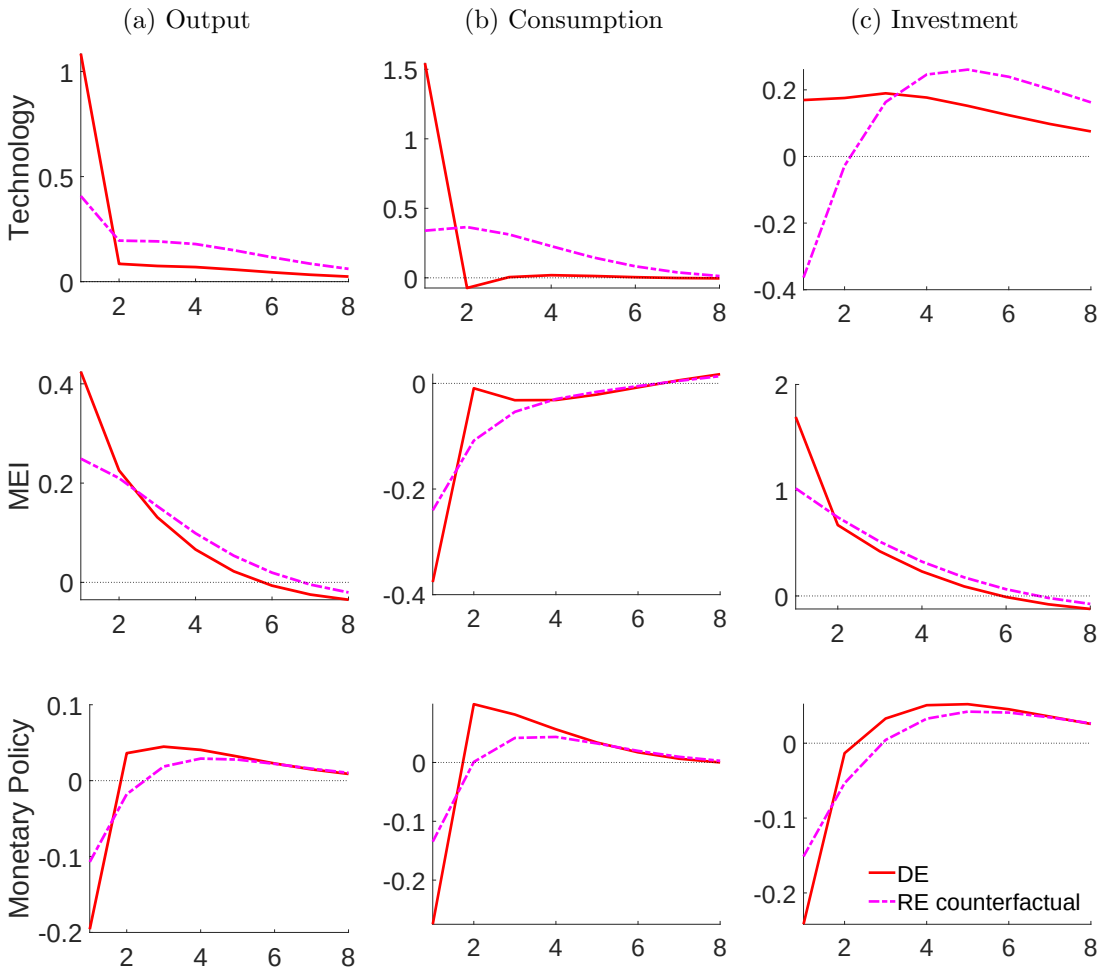

Notes: The panels depict the impulse responses of the growth rates of output, consumption, and investment to one-standard-deviation shocks to technology, MEI, and monetary policy. The red solid lines denote impulse responses under DE with RE forecast errors, whereas the magenta dash-dotted lines represent responses under the RE counterfactual. The responses are based on the posterior mean estimates of the parameters in the DE model with RE forecast errors; for the RE counterfactual, however, $\theta = 0$.

(output, consumption, and investment) to technology, MEI, and monetary policy shocks. The results reveal that DE generate amplified responses on impact, followed by rapid and immediate reversals. Such rich dynamics help improve the model's fit to the data.

However, in the DE model with DE forecast errors, shock propagation can be even more amplified and persistent than in the DE model with RE forecast errors. In particular, in response to a technology shock, investment strongly overreacts, triggering a rise in hours worked to sustain the elevated investment. These dynamics differ markedly from those in the competing models. Given the central role of technology shocks in business cycles, such excessive overreaction is at odds with the data, leading to the model's weaker empirical performance, as noted in the previous subsection.

Figure 5: Impulse Responses to Sunspot Shocks

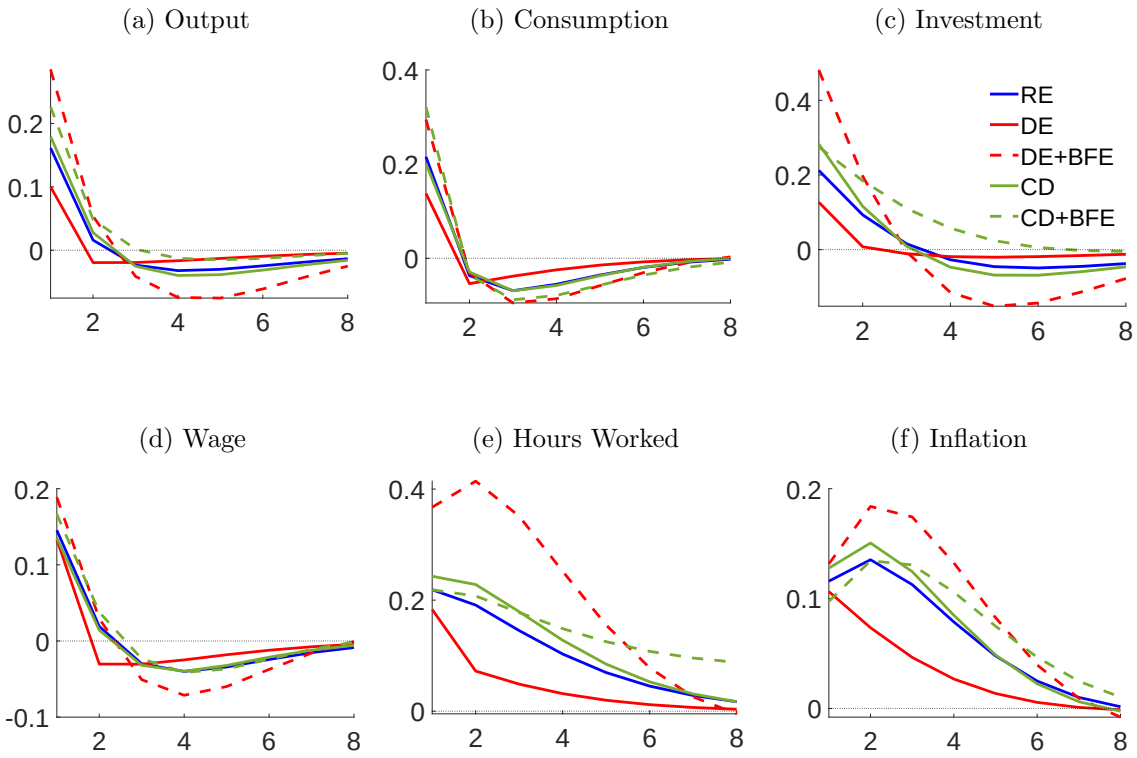

Notes: The panels depict the impulse responses of the growth rates of output, consumption, and investment, and wage; the level of hours worked; and the inflation rate to a one-standard-deviation shock to sunspot. The responses are based on the posterior mean estimates of parameters in each estimated model: the RE model, the DE model with RE forecast errors (DE), the DE model with DE forecast errors (DE+BFE), the CD model with RE forecast errors (CD), and the CD model with CD forecast errors (CD+BFE). see Table 2 for parameters.

Second, consider the dynamic responses in the CD models under RE- and CD-based forecast errors, respectively, shown in Figure 3. Section 2.1.3 analytically shows that CD with RE forecast errors generates more persistent propagation of shocks in the simple univariate model. However, the estimated medium-scale model under CD with RE forecast errors exhibits very similar responses across all observables compared to their RE counterparts, because the estimated CD parameter ($\phi = 0.976$) is close to the RE limit of 1.

In the univariate example, the dynamics under RE and under CD with CD forecast errors are identical (see Section 2.1.3 again). In contrast, in the medium-scale model with richer dynamic structures, the responses under CD with CD forecast errors diverge from those under RE. Given the estimated degree of CD ($\phi = 0.911$), the IRFs demonstrate more persistent dynamics, particularly hump-shaped patterns in wage and inflation. These realistic dynamics contribute to the better fit of the CD model with CD forecast errors relative to that with RE forecast errors, as discussed in Section 5.1.

Lastly, Figure 5 presents the IRFs to a one-standard-deviation sunspot shock in each model. In

our analysis, sunspot shocks are constructed following Lubik and Schorfheide (2004) and represent shifts in agents' beliefs that lead to positive changes in all expectational variables, independent of fundamentals. Under indeterminacy, such nonfundamental beliefs become self-fulfilling and influence actual variables in the same direction. Accordingly, the sunspot shock contemporaneously raises all observables shown in the figure across all specifications of expectation formation and forecast errors.

A notable difference across specifications emerges in the second period following the shock. Only the DE model with RE-based forecast errors exhibits reversal dynamics in output and wage, driving these variables into negative territory—a characteristic feature of DE models. In contrast, the DE model with DE-based forecast errors generates a continued rise in hours worked and displays highly persistent responses in all observables. The CD models yield dynamics that closely resemble those of the RE benchmark, regardless of the forecast error specification.

5.3 Variance Decomposition

Table 4 reports the forecast error variance decomposition at the infinite horizon for the observed variables used in the estimation: the growth rates of output, consumption, investment, and wage; the level of hours worked; the inflation rate; and the nominal interest rate. The decomposition quantifies the relative contribution of each structural shock—namely, technology, preference, MEI, external demand, wage markup, price markup, monetary policy, and sunspot shocks—to the variability of each observable under the five estimated models.

Under the benchmark RE model, technology shocks are the dominant driver of output and consumption growth, accounting for 50.9% and 69.5% of their variance, respectively, as is consistent with the majority of existing business cycle literature. Investment dynamics are largely driven by MEI shocks (67.9%) because investment-specific disturbances directly affect capital accumulation. Wage and price markups jointly explain a large portion of wage and inflation fluctuations. Notably, sunspot shocks account for more than half of inflation volatility (54.0%) and contribute significantly—approximately 10–20%—to the variability of the other observables. This pronounced role of sunspot shocks is a distinctive feature of the Japanese economy during the zero interest rate period, which likely induced equilibrium indeterminacy and sunspot fluctuations.

In the DE model with RE forecast errors, technology shocks play an even more prominent role—especially for output (58.0%) and consumption (75.7%)—owing to enhanced internal propagation of the technology shocks under DE. The overall pattern is broadly similar to that in the RE model, but the contribution of sunspot shocks is somewhat larger for wages (18.1%) and hours worked (22.6%).

A markedly different picture emerges under the DE model with DE forecast errors. In this case, preference shocks account for a larger share of the variance—particularly in consumption (16.5%)—reflecting their highly persistent effects on aggregate variables, as illustrated in Figure A1 in Appendix D. More significantly, the contribution of sunspot shocks increases substantially, explaining roughly 30–70% of the volatility in all observables. This finding is consistent with Figure

Table 4: Variance Decomposition

	$\Delta \log Y_t$	$\Delta \log C_t$	$\Delta \log I_t$	$\Delta \log W_t$	$\log l_t$	$\Delta \log P_t$	$\log R_t^n$
RE model:							
Technology	50.9	69.5	6.6	33.2	4.5	2.0	0.0
Preference	0.5	2.7	0.0	0.3	0.1	0.0	0.0
MEI	16.7	1.8	67.9	1.9	48.7	8.8	0.0
External demand	10.0	0.1	0.8	0.5	3.9	0.5	0.0
Wage markup	1.5	0.6	2.8	22.4	12.5	3.7	0.0
Price markup	8.1	4.8	12.5	29.7	13.7	30.1	0.0
Monetary policy	0.6	1.1	0.4	0.4	0.7	0.9	100.0
Sunspot	11.7	19.5	9.0	11.6	15.9	54.0	0.0
DE model:							
Technology	58.0	75.7	8.3	35.8	7.4	3.2	0.0
Preference	0.2	1.2	0.3	0.5	0.2	0.3	0.0
MEI	8.5	1.6	58.7	1.6	32.2	8.3	0.0
External demand	11.9	0.2	2.1	1.1	6.5	1.2	0.0
Wage markup	1.6	0.5	4.0	17.4	16.5	4.3	0.0
Price markup	6.7	2.8	15.1	24.1	12.5	25.7	0.0
Monetary policy	1.2	1.6	1.0	1.5	2.2	2.5	100.0
Sunspot	12.0	16.3	10.4	18.1	22.6	54.6	0.0
DE model with DE forecast errors:							
Technology	50.9	42.6	29.2	28.5	45.7	10.0	0.0
Preference	3.2	16.5	6.1	4.3	6.2	2.0	0.0
MEI	0.1	0.0	0.5	0.0	0.1	0.0	0.0
External demand	4.4	0.1	0.5	0.2	1.8	0.2	0.0
Wage markup	1.0	0.3	2.4	16.8	3.3	1.3	0.0
Price markup	4.5	2.3	9.1	20.2	6.6	13.7	0.0
Monetary policy	1.5	1.7	2.1	1.0	1.4	1.7	100.0
Sunspot	34.3	36.5	50.0	29.0	34.8	71.1	0.0
CD model:							
Technology	48.1	62.6	6.8	35.8	4.7	3.1	0.0
Preference	2.0	11.2	0.4	1.4	0.8	0.4	0.0
MEI	15.3	1.4	57.4	1.9	35.2	6.8	0.0
External demand	7.1	0.0	0.6	0.4	3.2	0.3	0.0
Wage markup	1.2	0.3	2.3	17.3	9.4	2.2	0.0
Price markup	7.9	3.5	13.4	29.4	15.0	24.4	0.0
Monetary policy	1.9	2.3	1.9	1.3	3.1	3.9	100.0
Sunspot	16.4	18.5	17.2	12.6	28.6	58.8	0.0
CD model with CD forecast errors:							
Technology	39.0	70.4	1.8	20.9	0.6	1.6	0.0
Preference	0.6	3.3	0.0	0.2	0.0	0.0	0.0
MEI	29.7	0.7	74.0	6.5	79.3	3.1	0.0
External demand	11.5	0.1	0.1	0.1	1.2	0.4	0.0
Wage markup	2.7	2.1	5.0	31.3	7.2	9.6	0.0
Price markup	11.7	12.5	15.6	38.1	9.4	68.9	0.0
Monetary policy	1.2	2.9	0.8	0.6	0.4	1.4	100.0
Sunspot	3.6	8.0	2.7	2.4	1.8	15.0	0.0

Note: This table shows the forecast error variance decomposition of the growth rates of output, consumption, investment, and wage; the level of hours worked; the inflation rate; and the nominal interest rate, at the infinite horizon, given the posterior mean estimates of parameters in each estimated model: the RE model, the DE model (with RE forecast errors), the DE model with DE forecast errors, the CD model (with RE forecast errors), and the CD model with CD forecast errors.

5 (Section 5.2), which shows that the DE model with DE forecast errors yields more pronounced and persistent effects across all variables.

In the CD model with RE forecast errors, the variance decomposition is broadly similar to that of the RE benchmark, as the two models exhibit closely aligned dynamic properties. Technology and MEI shocks again dominate fluctuations in real variables, while price markup shocks continue to account for a large share of the variance in wages (29.4%) and inflation (24.4%). Sunspot shocks contribute more to all observables, except consumption, than in the RE model.

Finally, the CD model with CD forecast errors reveals a substantial shift in the importance of MEI shocks, which now explain the majority of the variance in investment (74.0%) and hours worked (79.3%), and consequently a substantial portion of output (29.7%). The sharp rise in the role of MEI shocks aligns with the IRFs shown in Figure A1(b) in Appendix D, where the same specification generates stronger and more persistent responses across variables. Markup shocks account for the largest shares of the variance in wage and price dynamics. By contrast, sunspot shocks contribute much less to all observables than in the other specifications.

Overall, the variance decomposition underscores that the specifications of expectation formation and forecast errors fundamentally shape the model's shock transmission mechanisms. In all models with RE-based forecast errors, technology shocks dominate the variance of output, and sunspot shocks dominate that of inflation. In comparison, the DE and CD models, with their associated BE forecast errors, shift explanatory power toward sunspot shocks in the DE case and toward investment- or nominal-related disturbances in the CD case, thereby altering the sources of macroeconomic persistence and volatility to a significant degree.

5.4 Historical Decomposition

Figures 6 and 7 compare the historical decomposition of the output growth rate and the inflation rate, respectively, in terms of percentage deviations from the steady state, between the benchmark RE model and the "best-fit" DE model with RE forecast errors. For better visibility, the contributions of preference, MEI, external demand, and monetary policy shocks are aggregated as "demand" shocks, while those of wage and price markup shocks are combined as "markup" shocks. The results are based on the posterior mean estimates of the parameters in each estimated model.

The historical decomposition of output growth in the RE model (Figure 6(a)) demonstrates that technology shocks are the primary driver of fluctuations, consistent with the variance decomposition results presented in Table 4 in the previous subsection. Demand shocks also contribute substantially, particularly during the 2008–2009 global financial crisis, while the contributions of markup shocks are relatively modest. A notable finding is that sunspot shocks play a sizable role in offsetting large swings in output growth, especially during and after the global financial crisis and the COVID-19 pandemic. As Hirose (2020) argues, sunspot shocks may capture changes in expectations driven by the announcement and implementation of unconventional fiscal and monetary policy measures, which are not explicitly specified in the estimated model. These shocks are thus identified to contribute to stabilizing the economy during such periods.

Figure 6: Historical Decomposition of Output Growth

(a) RE model

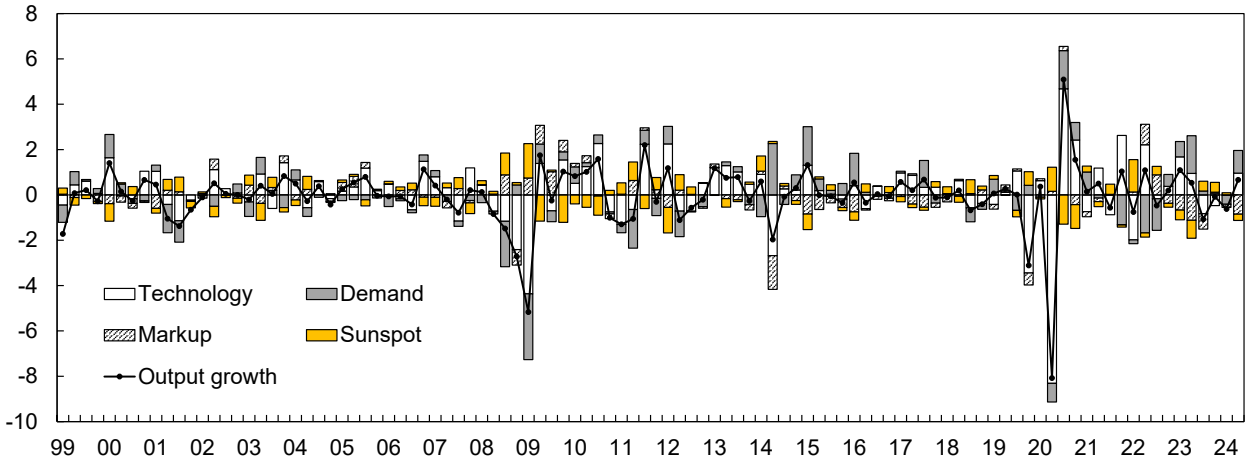

(b) DE model

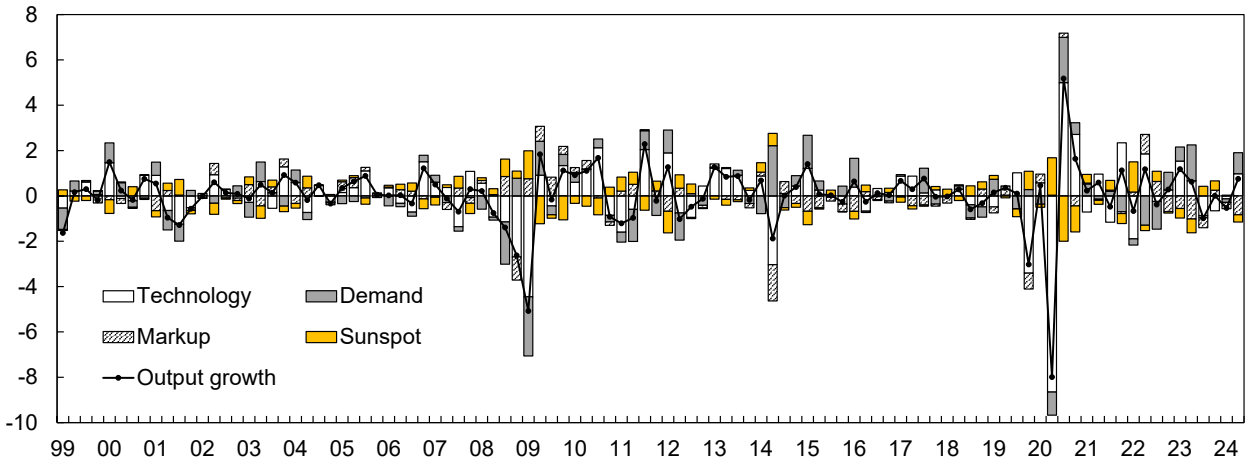

Notes: This figure shows the historical decomposition of the quarterly output growth rate in the RE model and the DE model with RE forecast errors, respectively, given the posterior mean estimates of the parameters. 'Demand' denotes the sum of the contributions of preference, MEI, external demand, and monetary policy shocks, whereas 'Markup' is the sum of the contributions of wage and price markup shocks.

The DE model with RE forecast errors (Figure 6(b)) exhibits an almost identical pattern, with technology shocks remaining the dominant driver of output growth fluctuations. Sunspot shocks continue to play a stabilizing role, albeit with a slightly increased contribution during the COVID-19 pandemic. During this period, the contribution of technology shocks becomes more pronounced, thereby increasing the offsetting role of sunspot shocks.

Regarding the historical decomposition of inflation, the RE model (Figure 7(a)) indicates that sunspot shocks and markup shocks are the primary drivers of inflation fluctuations over the sample period, consistent with the variance decomposition results in Table 4. Demand shocks also con-

Figure 7: Historical Decomposition of Inflation

(a) RE model

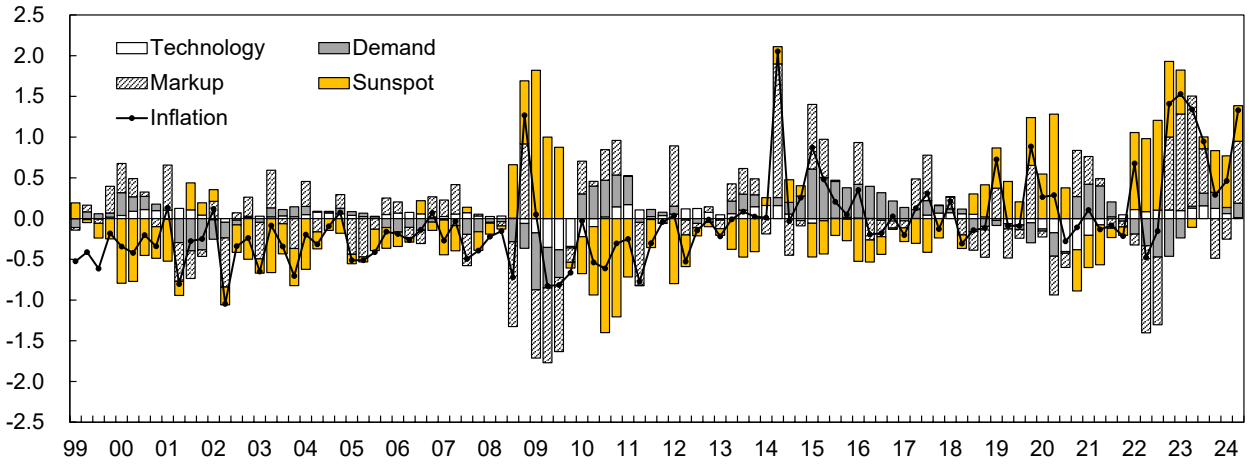

(b) DE model

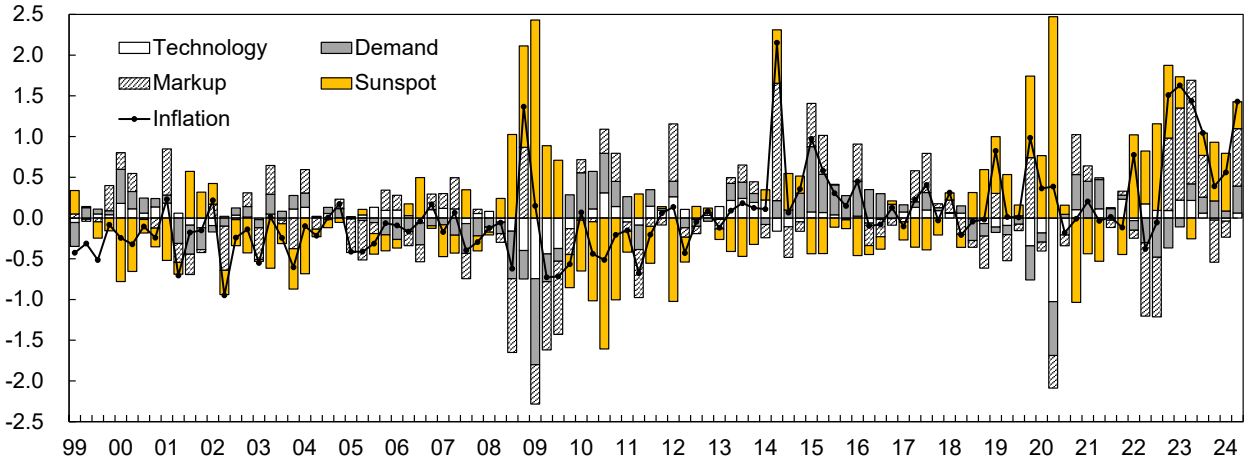

Notes: This figure shows the historical decomposition of the inflation rate in the RE model and the DE model with RE forecast errors, respectively, given the posterior mean estimates of the parameters. 'Demand' denotes the sum of the contributions of preference, MEI, external demand, and monetary policy shocks, whereas 'Markup' is the sum of the contributions of wage and price markup shocks.

tribute significantly, particularly in 2015 and 2016, when Japan's inflation began to rise steadily. A notable feature of sunspot shocks here is that, unlike their offsetting role in output growth, they occasionally amplify inflation fluctuations, especially during and after the global financial crisis and the COVID-19 pandemic. This suggests that sunspot shocks capture non-fundamental shifts in expectations that destabilized inflation during these episodes.

The DE model with RE forecast errors (Figure 7(b)) exhibits a similar pattern, with sunspot and markup shocks remaining the major sources of inflation variability. However, the contribution of technology shocks becomes more pronounced, particularly during the global financial crisis and the

COVID-19 pandemic, when they exert additional downward pressure on inflation. To counteract this, the contribution of sunspot shocks rises during these periods.

In summary, the historical decomposition shows that the RE model and the DE model with RE forecast errors yield broadly similar results for output growth and inflation, with technology shocks and sunspot shocks as the primary drivers of fluctuations in each, respectively. While sunspot shocks play a stabilizing role in output growth, they can amplify inflation volatility during periods of economic stress. The DE model, however, generates more pronounced effects of sunspot shocks, underscoring their importance in explaining business cycle dynamics in Japan.

6 Concluding Remarks

In this paper, we have investigated the quantitative implications and empirical relevance of BE within DSGE models under indeterminacy of equilibrium. In particular, we considered two leading BE frameworks—DE and CD—and compared their implications to the RE benchmark. Using a simple univariate model, we demonstrated that each expectation formation yields a distinct law of motion for the endogenous variable and generates different responses to both fundamental and sunspot shocks. To assess the empirical performance of these models, we estimated a medium-scale DSGE model for the Japanese economy during its prolonged zero interest rate period, a context in which indeterminacy is likely to prevail. The estimation results show that the DE model with RE-based forecast errors provides the best fit to the data, particularly in capturing the overreaction of aggregate variables to key exogenous shocks. Furthermore, variance and historical decompositions reveal that technology and markup shocks are the main drivers of output and inflation, respectively, while sunspot shocks contribute to output stabilization but amplify inflation volatility. Compared to the RE benchmark, the DE model assigns greater importance to sunspot shocks. Taken together, these findings underscore the importance of incorporating BE and accounting for indeterminacy in understanding macroeconomic fluctuations.

The following extensions are left for future work. While our analysis focused on DE and CD, it would be valuable to examine the quantitative and empirical implications of other BE specifications—such as adaptive expectations (Cagan, 1956; Friedman, 1957), sticky information (Mankiw and Reis, 2002), and overextrapolation (Angeletos et al., 2020)—in settings with indeterminacy. As Adams (2023) investigates extensively, the condition for determinacy can vary depending on the specific BE formulation. Therefore, our estimation approach, which allows for both determinacy and indeterminacy across the entire parameter space, offers a useful framework for estimating models with these alternative BE specifications.

Exploring a generalized formulation of DE—one that incorporates the distant past as a reference set, as proposed by Bianchi et al. (2024a) and its smoothed variant that links uncertainty to overreaction, as formalized in Bianchi et al. (2024b)—would also offer valuable insights into the interaction between these DE features and indeterminacy. For instance, when agents' selective memory recall is based on distant information, a new informational state—surprise—can emerge,

leading to richer dynamics such as repeated, endogenous cycles driven by the feedback loop between their actions and diagnostic beliefs. Under indeterminacy, this mechanism would further amplify the internal propagation of shocks emphasized in our analysis.

References

Adams, J. J. (2023): "Equilibrium Determinacy with Behavioral Expectations," Working Papers 001008, University of Florida, Department of Economics.

Afsar, A., J.-E. Gallegos, R. Jaimes, and E. Silgado-Gómez (2024): "A Behavioral Hybrid New Keynesian Model: Quantifying the Importance of Belief Formation Frictions," *Economic Modelling*, 132, 106626.

Angeletos, G.-M., Z. Huo, and K. A. Sastry (2020): "Imperfect Macroeconomic Expectations: Evidence and Theory," *NBER Macroeconomics Annual*, 35, 1–86.

Ascari, G. and T. Ropele (2009): "Trend Inflation, Taylor Principle and Indeterminacy," *Journal of Money, Credit and Banking*, 41, 1557–1584.

Beaudry, P. and A. Lahiri (2019): "The Unsettling Behavior of Exchange Rates Under Inflation Targeting," Unpublished manuscript, University of British Columbia.

Benchimol, J., L. Bounader, and M. Dotta (2025): "Estimating Behavioral Inattention," *Journal of Economic Behavior and Organization*, 236, 107068.

Bianchi, F., C. Ilut, and H. Saijo (2024a): "Diagnostic Business Cycles," *Review of Economic Studies*, 91, 129–162.

——— (2024b): "Smooth Diagnostic Expectations," NBER Working Paper 32152.

Blanchard, O. J. and C. M. Kahn (1980): "The Solution of Linear Difference Models under Rational Expectations," *Econometrica*, 48, 1305–1311.

Bordalo, P., N. Gennaioli, R. LaPorta, and A. Shleifer (2019): "Diagnostic Expectations and Stock Returns," *Journal of Finance*, 74, 2839–2874.

Bordalo, P., N. Gennaioli, Y. Ma, and A. Shleifer (2020): "Overreaction in Macroeconomic Expectations," *American Economic Review*, 110, 2748–82.

Bordalo, P., N. Gennaioli, and A. Shleifer (2018): "Diagnostic Expectations and Credit Cycles," *Journal of Finance*, 73, 199–227.

Bordalo, P., N. Gennaioli, A. Shleifer, and S. J. Terry (2021): "Real Credit Cycles," *NBER Working Paper No. 28416*.

Cagan, P. (1956): "The Monetary Dynamics of Hyperinflation," in *Studies in the Quantity Theory of Money*, ed. by M. Friedman, Chicago: The University of Chicago Press, 25–117.

Calvo, G. A. (1983): "Staggered Prices in a Utility-Maximizing Framework," *Journal of Monetary Economics*, 12, 383–398.

Carlstrom, C. T. and T. S. Fuerst (1997): "Agency Costs, Net Worth, and Business Fluctuations: A Computable General Equilibrium Analysis," *American Economic Review*, 87, 893–910.

Christiano, L. J., M. Eichenbaum, and C. L. Evans (2005): "Nominal Rigidities and the Dynamic Effects of a Shock to Monetary Policy," *Journal of Political Economy*, 113, 1–45.

Coibion, O. and Y. Gorodnichenko (2011): "Monetary Policy, Trend Inflation, and the Great Moderation: An Alternative Interpretation," *American Economic Review*, 101, 341–370.

D'Arienzo, D. (2020): "Maturity Increasing Overreaction and Bond Market Puzzles," Mimeo, Bocconi University.

Erceg, C. J., L. Guerrieri, and C. Gust (2006): "SIGMA: A New Open Economy Model for Policy Analysis," *International Journal of Central Banking*, 2, 1–50.

Friedman, M. (1957): *A Theory of the Consumption Function*, Princeton: Princeton University Press.

Fujiwara, I. and Y. Hirose (2024): "Connecting Exchange Rates to Fundamentals Under Indeterminacy," CEPR Discussion Papers 19744.

Gabaix, X. (2020): "A Behavioral New Keynesian Model," *American Economic Review*, 110, 2271–2327.

Greenwood, J., Z. Hercowitz, and G. W. Huffman (1988): "Investment, Capacity Utilization, and the Real Business Cycle," *American Economic Review*, 78, 402–417.

Herbst, E. and F. Schorfheide (2014): "Sequential Monte Carlo Sampling for DSGE Models," *Journal of Applied Econometrics*, 29, 1073–1098.

——— (2015): *Bayesian Estimation of DSGE Models*, Princeton University Press.

Hirose, Y. (2020): "An Estimated DSGE Model with a Deflation Steady State," *Macroeconomic Dynamics*, 24, 1151–1185.

Hirose, Y., H. Iiboshi, M. Shintani, and K. Ueda (2024): "Estimating a Behavioral New Keynesian Model with the Zero Lower Bound," *Journal of Money, Credit and Banking*, 56, 2185–2197.

Hirose, Y., T. Kurozumi, and W. Van Zandweghe (2020): "Monetary Policy and Macroeconomic Stability Revisited," *Review of Economic Dynamics*, 37, 255–274.

Hirose, Y., T. Kurozumi, and W. V. Zandweghe (2023): "Inflation Gap Persistence, Indeterminacy, and Monetary Policy," *Review of Economic Dynamics*, 51, 867–887.

Ilabaca, F. and G. Meggiorini (2023): "Trend Inflation Under Bounded Rationality," Working Papers 23-09, Office of Financial Research, US Department of the Treasury.

Ilabaca, F., G. Meggiorini, and F. Milani (2020): "Bounded Rationality, Monetary Policy, and Macroeconomic Stability," *Economics Letters*, 186, 108522.

Iwasaki, Y., I. Muto, and M. Shintani (2021): "Missing Wage Inflation? Estimating the Natural Rate of Unemployment in a Nonlinear DSGE Model," *European Economic Review*, 132, 103626.

Justiniano, A., G. Primiceri, and A. Tambalotti (2010): "Investment Shocks and Business Cycles," *Journal of Monetary Economics*, 57, 132–145.

Klein, P. (2000): "Using the Generalized Schur Form to Solve a Multivariate Linear Rational Expectations Model," *Journal of Economic Dynamics and Control*, 24, 1405–1423.

L'Huillier, J.-P., S. R. Singh, and D. Yoo (2024): "Incorporating Diagnostic Expectations into the New Keynesian Framework," *The Review of Economic Studies*, 91, 3013–3046.

Lubik, T. A. and F. Schorfheide (2003): "Computing Sunspot Equilibria in Linear Rational Expectations Models," *Journal of Economic Dynamics and Control*, 28, 273–285.

——— (2004): "Testing for Indeterminacy: An Application to U.S. Monetary Policy," *American Economic Review*, 94, 190–217.

Mankiw, G. and R. Reis (2002): "Sticky Information Versus Sticky Prices: A Proposal to Replace the New Keynesian Phillips Curve," *Quarterly Journal of Economics*, 117, 1295–1328.

Meggiorini, G. (2023): "Behavioral New Keynesian Models: An Empirical Assessment," *Journal of Macroeconomics*, 77, 103538.

Meggiorini, G. and F. Milani (2021): "Behavioral New Keynesian Models: Learning vs. Cognitive Discounting," CESifo Working Paper Series 9039, CESifo.

Na, S. and D. Yoo (2025): "Overreaction and Macroeconomic Fluctuation of the External Balance," *Journal of Monetary Economics*, 151, 103750.

Pflueger, C., E. Siriwardane, and A. Sunderam (2020): "Financial Market Risk Perceptions and the Macroeconomy," *Quarterly Journal of Economics*, 135, 1443–1491.

Rotemberg, J. J. (1982): "Sticky Prices in the United States," *Journal of Political Economy*, 90, 1187–1211.

Sims, C. A. (2002): "Solving Linear Rational Expectations Models," *Computational Economics*, 20, 1–20.

Smets, F. and R. Wouters (2007): "Shocks and Frictions in US Business Cycles: A Bayesian DSGE Approach," *American Economic Review*, 97, 586–606.

Sugo, T. and K. Ueda (2008): "Estimating a Dynamic Stochastic General Equilibrium Model for Japan," *Journal of the Japanese and International Economies*, 22, 476–502.

Appendix

A Stability of Canonical Systems in the Simple Example

A.1 Canonical system under DE with RE-based forecast errors

Given the canonical form (11):

$$\begin{bmatrix} 1 & 0 \\ 1 & 0 \end{bmatrix} \begin{bmatrix} \mathbb{E}_t y_{t+1} \\ \mathbb{E}_t y_{t+2} \end{bmatrix} = \begin{bmatrix} \frac{\alpha}{1+\theta} & \frac{\theta}{1+\theta} \\ 0 & 1 \end{bmatrix} \begin{bmatrix} \mathbb{E}_{t-1} y_t \\ \mathbb{E}_{t-1} y_{t+1} \end{bmatrix} + \begin{bmatrix} -\frac{\alpha}{1+\theta} \\ 0 \end{bmatrix} \varepsilon_t + \begin{bmatrix} \frac{\alpha}{1+\theta} & 0 \\ 0 & 1 \end{bmatrix} \begin{bmatrix} \eta_{1,t} \\ \eta_{2,t} \end{bmatrix},$$

let

$$\Gamma_0 = \begin{bmatrix} 1 & 0 \\ 1 & 0 \end{bmatrix}, \quad \Gamma_1 = \begin{bmatrix} \frac{\alpha}{1+\theta} & \frac{\theta}{1+\theta} \\ 0 & 1 \end{bmatrix}.$$

Then, the generalized eigenvalue λ of the system can be derived by solving the following characteristic equation:

$$\begin{aligned} & \det(\lambda\Gamma_0 - \Gamma_1) = 0 \\ \Leftrightarrow & \begin{vmatrix} \lambda - \frac{\alpha}{1+\theta} & -\frac{\theta}{1+\theta} \\ \lambda & -1 \end{vmatrix} = 0 \\ \Leftrightarrow & \frac{1}{1+\theta}(-\lambda + \alpha) = 0 \\ \Rightarrow & \lambda = \alpha. \end{aligned}$$

Therefore, α determines the stability property of the system.

A.2 Canonical system under DE with BE-based forecast errors

Given the canonical form (14):

$$\begin{bmatrix} 1 & 0 & 0 \\ 1 & 0 & 0 \\ 0 & 0 & 1 \end{bmatrix} \begin{bmatrix} \mathbb{E}_t y_{t+1} \\ \mathbb{E}_t y_{t+2} \\ \mathbb{E}_{t-1} y_{t+1} \end{bmatrix} = \begin{bmatrix} \alpha & \frac{\theta}{1+\theta} & -\frac{\alpha\theta}{1+\theta} \\ 0 & 1 & 0 \\ 0 & 1 & 0 \end{bmatrix} \begin{bmatrix} \mathbb{E}_{t-1} y_t \\ \mathbb{E}_{t-1} y_{t+1} \\ \mathbb{E}_{t-2} y_t \end{bmatrix} + \begin{bmatrix} -\frac{\alpha}{1+\theta} \\ 0 \\ 0 \end{bmatrix} \varepsilon_t + \begin{bmatrix} \frac{\alpha}{1+\theta} & 0 \\ 0 & 1 \\ 0 & 0 \end{bmatrix} \begin{bmatrix} \eta_{1,t} \\ \eta_{2,t} \end{bmatrix},$$

let

$$\Gamma_0 = \begin{bmatrix} 1 & 0 & 0 \\ 1 & 0 & 0 \\ 0 & 0 & 1 \end{bmatrix}, \quad \Gamma_1 = \begin{bmatrix} \alpha & \frac{\theta}{1+\theta} & -\frac{\alpha\theta}{1+\theta} \\ 0 & 1 & 0 \\ 0 & 1 & 0 \end{bmatrix}$$

Then, the generalized eigenvalues λ of the system can be derived by solving the following

characteristic equation:

$$
\begin{aligned}
&\det(\lambda\Gamma_0 - \Gamma_1) = 0 \\
&\Leftrightarrow \begin{vmatrix} \lambda-\alpha & -\frac{\theta}{1+\theta} & \frac{\alpha\theta}{1+\theta} \\ \lambda & -1 & 0 \\ 0 & -1 & \lambda \end{vmatrix} = 0 \\
&\Leftrightarrow (\lambda-\alpha)\begin{vmatrix} -1 & 0 \\ -1 & \lambda \end{vmatrix} + \left(-\left(-\frac{\theta}{1+\theta}\right)\right)\begin{vmatrix} \lambda & 0 \\ 0 & \lambda \end{vmatrix} + \frac{\alpha\theta}{1+\theta}\begin{vmatrix} \lambda & -1 \\ 0 & -1 \end{vmatrix} = 0 \\
&\Leftrightarrow \frac{\lambda}{1+\theta}(-\lambda+\alpha) = 0 \\
&\Rightarrow \lambda_1 = 0, \quad \lambda_2 = \alpha.
\end{aligned}
$$

As the zero eigenvalue corresponds to the unit root of the identity equation for $\mathbb{E}_{t-1}y_{t+1}$, the stability of the system is solely governed by α.

B Equilibrium Conditions of the Medium-Scale Model

B.1 First order conditions for households and firms

B.1.1 Households

In the presence of complete insurance markets, the decisions are the same for all households, and hence the first-order conditions with respect to consumption, bond-holdings, wage, capital utilization, investment, and capital stock are given by

$$\Lambda_t = e^{z_t^b}\left(C_t - \gamma C_{t-1}\right)^{-\sigma} - \beta\gamma\mathbb{E}_t^* e^{z_{t+1}^b}\left(C_{t+1} - \gamma C_t\right)^{-\sigma},$$

$$\Lambda_t = \beta\mathbb{E}_t^*\Lambda_{t+1}\frac{R_t^n}{\pi_{t+1}},$$

$$
\begin{aligned}
&e^{z_t^b}\left(\frac{1}{\lambda_t^w}+1\right)Z_t^{1-\sigma}l_t^{1+\chi} = \Lambda_t\left\{1 - \frac{\varphi_w}{2}\left(\pi_t\frac{W_t}{W_{t-1}\pi z} - 1\right)^2\right\}\frac{1}{\lambda_t^w}l_t W_t \\
&+ \varphi_w\Lambda_t\left(\pi_t\frac{W_t}{W_{t-1}\pi z} - 1\right)\pi_t\frac{W_t}{W_{t-1}\pi z}l_t W_t - \beta\varphi_w\mathbb{E}_t^*\Lambda_{t+1}\left(\pi_{t+1}\frac{W_{t+1}}{W_t\pi z} - 1\right)\pi_{t+1}\frac{W_{t+1}}{W_t\pi z}l_{t+1}W_{t+1},
\end{aligned}
$$

$$R_t^k = q_t\delta'(u_t),$$

$$
\begin{aligned}
1 = q_t e^{z_t^i}&\left\{1 - S\left(\frac{I_t}{I_{t-1}z}\right) - S'\left(\frac{I_t}{I_{t-1}z}\right)\frac{I_t}{I_{t-1}z}\right\} + \beta\mathbb{E}_t^*\frac{\Lambda_{t+1}}{\Lambda_t}q_{t+1}e^{z_{t+1}^i}S'\left(\frac{I_{t+1}}{I_t z}\right)\left(\frac{I_{t+1}}{I_t}\right)^2\frac{1}{z},
\end{aligned}
$$

$$q_t = \mathbb{E}_t^*\,\beta\frac{\Lambda_{t+1}}{\Lambda_t}\left\{R_{t+1}^k u_{t+1} + q_{t+1}\left(1 - \delta(u_{t+1})\right)\right\},$$

where Λ_t is the Lagrange multiplier interpreted as the marginal utility of income, $\pi_t = P_t/P_{t-1}$ is the gross inflation rate, and q_t is the real price of capital in terms of marginal utility.

B.1.2 Firms

Final-good firm The first-order condition for profit maximization yields the final-good firm's demand for each intermediate good given by $Y_t(f) = Y_t(P_t(f)/P_t)^{-(1+\lambda_t^p)/\lambda_t^p}$, while perfect competition in the final-good market leads to its price P_t, given by

$$P_t = \left(\int_0^1 P_t(f)^{-\frac{1}{\lambda_t^p}} df \right)^{-\lambda_t^p}.$$

Intermediate-good firms Combining cost-minimizing conditions with respect to capital and labor services shows that the real marginal cost is identical across intermediate-good firms and is given by

$$mc_t = \left(\frac{W_t}{(1-\alpha)Z_t} \right)^{1-\alpha} \left(\frac{R_t^k}{\alpha} \right)^{\alpha}.$$

Furthermore, combining the cost-minimizing conditions and aggregating the resulting equation over intermediate-good firms shows that the capital–labor ratio is identical across intermediate-good firms and is given by

$$\frac{u_t K_{t-1}}{l_t} = \frac{\alpha W_t}{(1-\alpha)R_t^k},$$

where $K_t = \int_0^1 K_t(f)df$ and $l_t = \int_0^1 l_t(f)df$.

Under the symmetric equilibrium, *i.e.*, $P_t(f) = P_t$, the first-order condition for each intermediate-good firm's profit maximization leads to

$$0 = \left\{ 1 - \varphi_p \left(\frac{\pi_t}{\pi_{t-1}^{\gamma_p} \pi^{1-\gamma_p}} - 1 \right) \frac{\pi_t}{\pi_{t-1}^{\gamma_p} \pi^{1-\gamma_p}} \right\} Y_t \lambda_t^p - \frac{1+\lambda_t^p}{\lambda_t^p} \left\{ 1 - mc_t - \frac{\varphi_p}{2} \left(\frac{\pi_t}{\pi_{t-1}^{\gamma_p} \pi^{1-\gamma_p}} - 1 \right)^2 \right\} Y_t$$
$$+ \beta \varphi_p \mathbb{E}_t^* \frac{\Lambda_{t+1}}{\Lambda_t} \left(\frac{\pi_{t+1}}{\pi_t^{\gamma_p} \pi^{1-\gamma_p}} - 1 \right) \frac{\pi_{t+1}}{\pi_t^{\gamma_p} \pi^{1-\gamma_p}} Y_{t+1}.$$

B.2 Detrended Equilibrium Conditions and Steady-State Relationships

The detrended equilibrium conditions of the model are given by the following equations:

$$\lambda_t = e^{z_t^b} \left(c_t - \gamma z_{t-1}^{-1} c_{t-1} \right)^{-\sigma} - \beta \gamma \mathbb{E}_t^* e^{z_{t+1}^b} \left(c_{t+1} z_{t+1} - \gamma c_t \right)^{-\sigma},$$

$$\lambda_t = \beta \mathbb{E}_t^* \lambda_{t+1} z_{t+1}^{-\sigma} \frac{R_t^n}{\pi_{t+1}},$$

$$
\begin{aligned}
e^{z_t^b}(\frac{1}{\lambda_t^w}+1)l_t^{1+\chi} &= \lambda_t\left\{1-\frac{\varphi_w}{2}\left(\pi_t\frac{w_t}{w_{t-1}\pi z}z_t-1\right)^2\right\}\frac{1}{\lambda_t^w}l_t w_t \\
&+\varphi_w\lambda_t\left\{\pi_t\frac{w_t}{w_{t-1}\pi z}z_t-1\right\}\pi_t\frac{w_t}{w_{t-1}\pi z}z_t l_t w_t \\
&-\beta\varphi_w\mathbb{E}_t^*\lambda_{t+1}z_{t+1}^{-\sigma}\left\{\pi_{t+1}\frac{w_{t+1}}{w_t\pi z}z_{t+1}-1\right\}\pi_{t+1}\frac{w_{t+1}}{w_t\pi z}z_{t+1}l_{t+1}w_{t+1}z_{t+1},
\end{aligned}
$$

$$
R_t^k = q_t\delta'(u_t),
$$

$$
\begin{aligned}
1 &= q_t e^{z_t^i}\left\{1-S\left(\frac{i_t}{i_{t-1}z}z_t\right)-S'\left(\frac{i_t}{i_{t-1}z}z_t\right)\frac{i_t}{i_{t-1}z}z_t\right\} \\
&+\beta\mathbb{E}_t^*\frac{\lambda_{t+1}}{\lambda_t}z_t^{-\sigma}q_{t+1}e^{z_{t+1}^i}S'\left(\frac{i_{t+1}}{i_t z}z_{t+1}\right)\left(\frac{i_{t+1}}{i_t}z_t\right)^2\frac{1}{z},
\end{aligned}
$$

$$
q_t = \beta\mathbb{E}_t^*\frac{\lambda_{t+1}}{\lambda_t}z_{t+1}^{-\sigma}\left\{R_{t+1}^k u_{t+1}+q_{t+1}\left(1-\delta(u_{t+1})\right)\right\},
$$

$$
k_t = \left\{1-\delta(u_t)\right\}k_{t-1}z_t^{-1}+e^{z_t^i}\left\{1-S\left(\frac{i_t}{i_{t-1}z}z_t\right)\right\}i_t,
$$

$$
y_t = c_t+i_t+de^{z_t^d}+\frac{\varphi_p}{2}\left(\frac{\pi_t}{\pi_{t-1}^{\gamma_p}\pi^{1-\gamma_p}}-1\right)^2 y_t,
$$

$$
mc_t = \left(\frac{w_t}{1-\alpha}\right)^{1-\alpha}\left(\frac{R_t^k}{\alpha}\right)^{\alpha},
$$

$$
\frac{u_t k_{t-1}}{l_t z_t} = \frac{\alpha w_t}{(1-\alpha)R_t^k},
$$

$$
\begin{aligned}
0 &= \left\{1-\varphi_p\left(\pi_t\pi_{t-1}^{-\gamma_p}\pi^{-1+\gamma_p}-1\right)\pi_t\pi_{t-1}^{-\gamma_p}\pi^{-1+\gamma_p}\right\}y_t \\
&-\left(\frac{1}{\lambda_t^p}+1\right)\left\{1-mc_t-\frac{\varphi_p}{2}\left(\pi_t\pi_{t-1}^{-\gamma_p}\pi^{-1+\gamma_p}-1\right)^2\right\}y_t \\
&+\beta\mathbb{E}_t^*\frac{\lambda_{t+1}}{\lambda_t}z_{t+1}^{-\sigma}\phi_p\left(\pi_{t+1}\pi_t^{-\gamma_p}\pi^{-1+\gamma_p}-1\right)\pi_{t+1}\pi_t^{-\gamma_p}\pi^{-1+\gamma_p}y_{t+1}z_{t+1}.
\end{aligned}
$$

The steady-state relationships are given by

$$
\begin{aligned}
\beta &= \frac{z^\sigma}{R}, \\
R^k &= R-1+\delta, \\
w &= (1-\alpha)\left(\frac{1}{1+\lambda^p}\right)^{\frac{1}{1-\alpha}}\left(\frac{R^k}{\alpha}\right)^{-\frac{\alpha}{1-\alpha}}, \\
\frac{k}{l} &= \frac{\alpha z w}{(1-\alpha)R^k},
\end{aligned}
$$

$$
\begin{aligned}
\varphi_y &= \lambda^p, \\
\frac{k}{y} &= (1+\varphi_y) z^{\alpha} \left(\frac{k}{l}\right)^{1-\alpha}, \\
\frac{i}{y} &= \left(1 - \frac{1-\delta}{z}\right)\frac{k}{y}, \\
\frac{c}{y} &= 1 - \frac{i}{y} - \frac{d}{y}.
\end{aligned}
$$

C Sequential Monte Carlo Algorithm

To approximate the posterior distribution of model parameters, we employ a generic SMC algorithm with likelihood tempering, as described in Herbst and Schorfheide (2014, 2015). In the algorithm, a sequence of tempered posteriors is defined as

$$
\varpi_n(\boldsymbol{\theta}) = \frac{[p(\mathbf{Y}^T|\boldsymbol{\theta},\mathbf{M})]^{\tau_n} p(\boldsymbol{\theta},\mathbf{M})}{\int [p(\mathbf{Y}^T|\boldsymbol{\theta},\mathbf{M})]^{\tau_n} p(\boldsymbol{\theta},\mathbf{M}) d\boldsymbol{\theta} d\mathbf{M}}, \quad n = 0, ..., N_\tau,
$$

where N_τ denotes the number of stages and is set at $N_\tau = 200$. The tempering schedule $\{\tau_n\}_{n=0}^{N_\tau}$ is determined by $\tau_n = (n/N_\tau)^\mu$, where μ is a parameter that controls the shape of the tempering schedule and is set at $\mu = 2$, following Herbst and Schorfheide (2014, 2015). The SMC algorithm generates parameter draws $\{\boldsymbol{\theta}_n^{(i)}, \mathbf{M}_n^{(i)}\}$ and associated importance weights $w_n^{(i)}$, called particles, from the sequence of posteriors $\{\varpi_n\}_{n=1}^{N_\tau}$; *i.e.*, at each stage, $\varpi_n(\boldsymbol{\theta})$ is represented by a swarm of particles $\{\boldsymbol{\theta}_n^{(i)}, \mathbf{M}_n^{(i)}, w_n^{(i)}\}_{i=1}^{N}$, where N denotes the number of particles. In the subsequent estimation, the algorithm uses $N = 10,000$ particles. For $n = 0, ..., N_\tau$, the algorithm sequentially updates the swarm of particles $\{\boldsymbol{\theta}_n^{(i)}, \mathbf{M}_n^{(i)}, w_n^{(i)}\}_{i=1}^{N}$ through importance sampling.[16]

Posterior inferences on model parameters are made based on the particles $\{\boldsymbol{\theta}_{N_\tau}^{(i)}, \mathbf{M}_{N_\tau}^{(i)}, w_{N_\tau}^{(i)}\}_{i=1}^{N}$ from the final importance sampling. The SMC-based approximation of the marginal data density is given by

$$
p(\mathbf{Y}^T) = \prod_{n=1}^{N_\tau} \left(\frac{1}{N} \sum_{i=1}^{N} \tilde{w}_n^{(i)} w_{n-1}^{(i)} \right),
$$

where $\tilde{w}_n^{(i)}$ is the incremental weight defined as $\tilde{w}_n^{(i)} = [p(\mathbf{Y}^T|\boldsymbol{\theta}_{n-1}^{(i)}, \mathbf{M}_{n-1}^{(i)})]^{\tau_n - \tau_{n-1}}$. The posterior probability of equilibrium determinacy can be calculated as

$$
\mathbb{P}\{\boldsymbol{\theta} \in \boldsymbol{\Theta}^D | \mathbf{Y}^T\} = \frac{1}{N} \sum_{i=1}^{N} \mathbf{1}\{\boldsymbol{\theta}_{N_\tau}^{(i)} \in \boldsymbol{\Theta}^D\}.
$$

Likewise, the prior probability of equilibrium determinacy can be computed using prior draws.

[16] This process includes one step of a single-block random-walk Metropolis–Hastings algorithm.

D Additional Impulse Responses

Figure A1 presents the IRFs for the growth rates of output, consumption, investment, and wage, as well as the level of hours worked and the inflation rate (and the nominal interest rate for a monetary policy shock) to one-standard-deviation shocks about preferences, MEI, external demand, wage markups, price markups, and monetary policy. The responses are expressed as percentage deviations from their steady-state values and are based on the posterior mean estimates of parameters in each estimated model: the RE model (blue solid lines), the DE model with RE forecast errors (red solid lines), the DE model with DE forecast errors (red dashed lines), the CD model with RE forecast errors (green solid lines), and the CD model with CD forecast errors (green dashed lines).

Figure A1: Impulse Responses to Structural Shocks

(a) Preference Shock

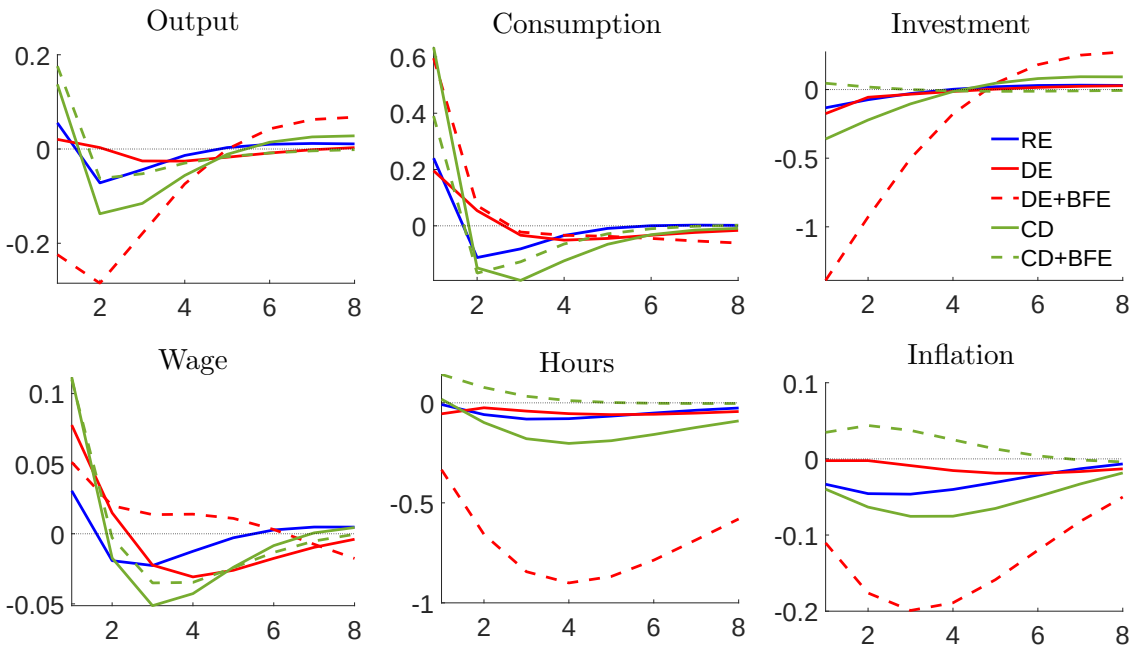

(b) MEI Shock

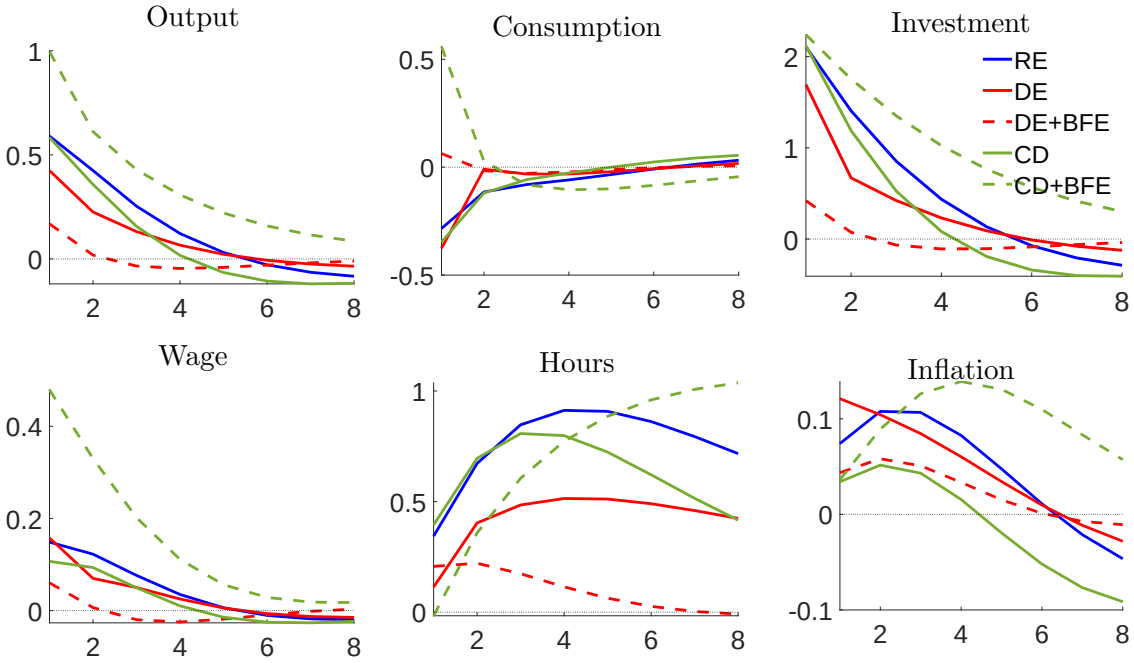

Figure A1: Impulse Responses to Structural Shocks (continued)

(c) External Demand Shock

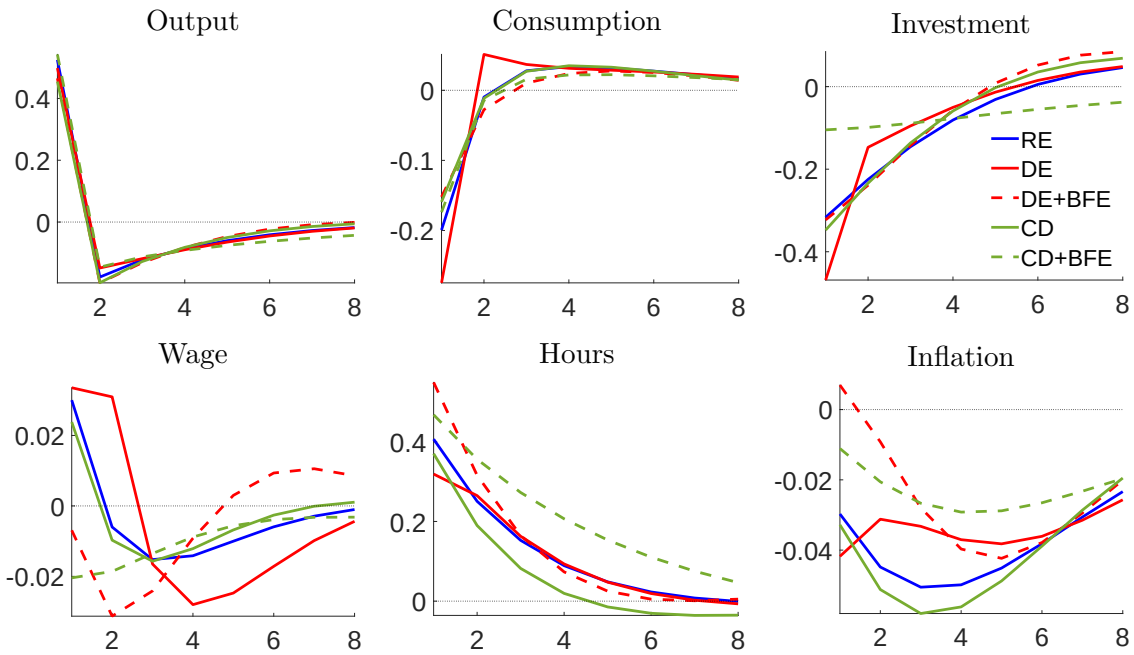

(d) Wage Markup Shock

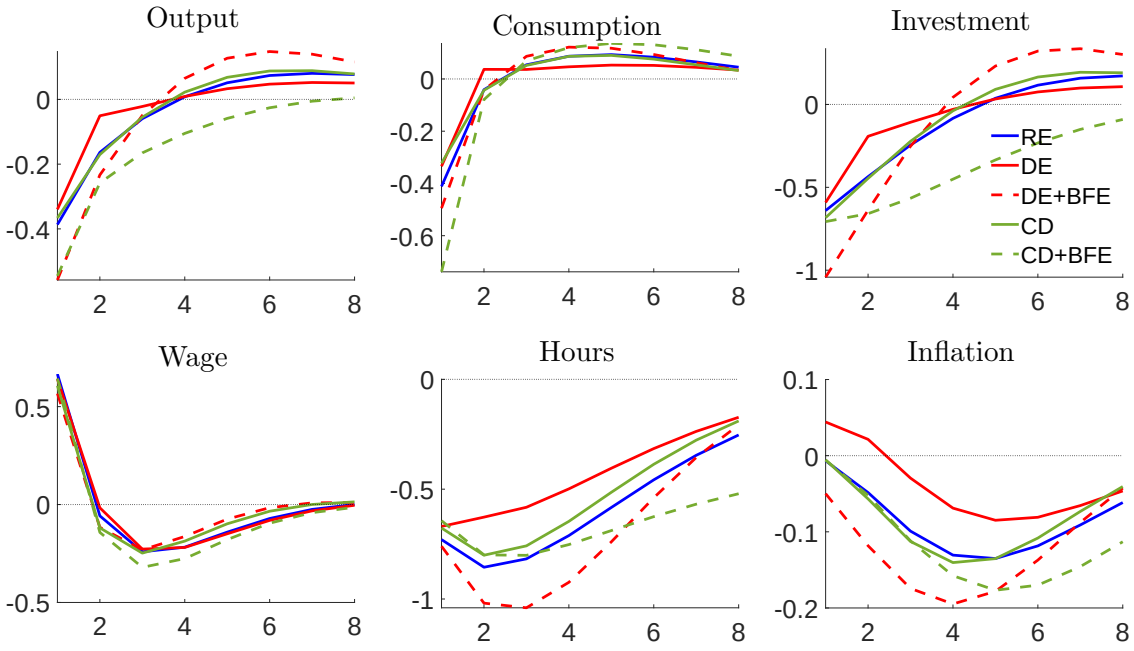

Figure A1: Impulse Responses to Structural Shocks (continued)

(e) Price Markup Shock

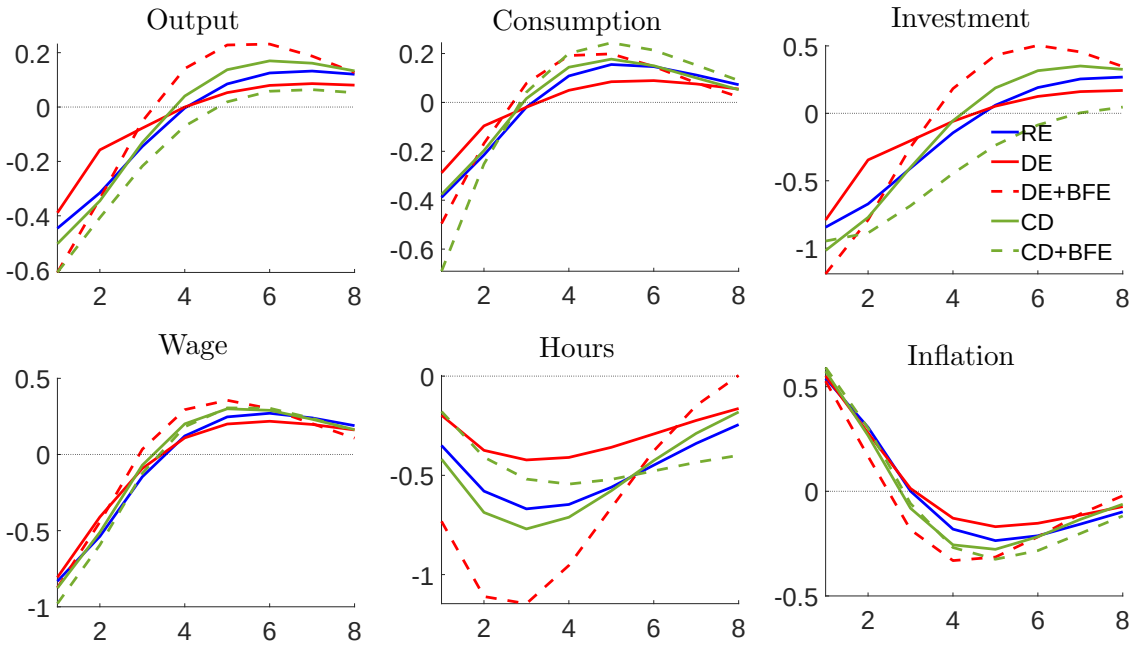

Figure A1: Impulse Responses to Structural Shocks (continued)

(f) Monetary Policy Shock

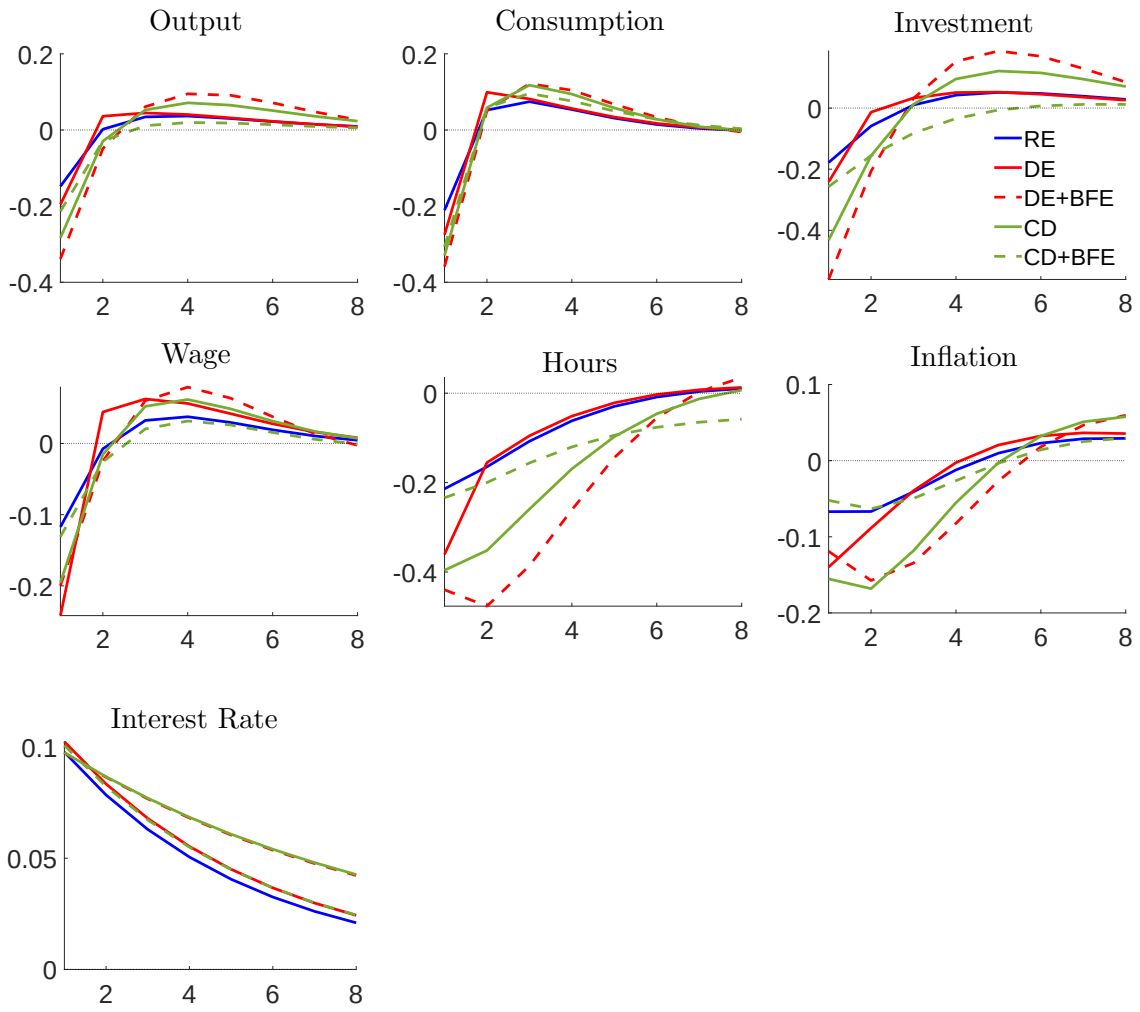

Notes: The panels depict the impulse responses for the growth rates of output, consumption, and investment, and wage; the level of hours worked; and the inflation rate (and the nominal interest rate for the monetary policy shock) to one-standard-deviation shocks to preference, MEI, external demand, wage markup, price markup, and monetary policy. The responses are based on the posterior mean estimates of parameters in each estimated model: the RE model, the DE model with RE forecast errors (DE), the DE model with DE forecast errors (DE+BFE), the CD model with RE forecast errors (CD), and the CD model with CD forecast errors (CD+BFE).